UNIVERSITÀ DEGLI STUDI DELL'INSUBRIA

Dottorato di ricerca XXV ciclo in

"Fisiologia Sperimentale e Clinica"

Scuola di Dottorato in

"Scienze Biologiche e Mediche"

DIPARTIMENTO DI BIOTECNOLOGIE E SCIENZE DELLA VITA

Laboratorio di Fisiologia Cellulare e Molecolare

PROPERTIES OF THE INSECT NEUTRAL AMINO ACID COTRANSPORTER KAAT1 STUDIED BY ALANINE SCANNING MUTAGENESIS AND TEMPERATURE

Tutor:
Dott.ssa Elena Bossi

Coordinatore:
Prof.ssa Daniela Negrini

Dottoranda:

Dott.ssa Francesca D'Antoni

2009 - 2012

Ai miei affetti più cari.

"Il cervello: se lo coltivi funziona. Se lo lasci andare e lo metti in pensione si indebolisce. La sua plasticità è formidabile. Per questo bisogna continuare a pensare".

Rita Levi Montalcini

Summary

The possibility of heterologous expression in *Xenopus laevis* oocytes has greatly expanded the knowledge of the properties of several cotransporters, membrane proteins that, combining features of pumps and channels, couple the movement of ions and substrates. Transport across the membrane guarantees the reuptake of neurotransmitters from the synaptic cleft, the absorption of nutrients, the regulation of osmolarity and ionic homeostasis. Some of these proteins are involved in neurological diseases and in drug abuse. All the Na^+/Cl^--dependent cotransporters share high homology and possess the structural topology of the procariotic prototype transporter, LeuT. The present research work was focused on the insect neutral amino acid contransporter KAAT1 (K^+-coupled Amino Acid Transporter 1), cloned from the midgut of the larva of *Manduca sexta* (Castagna *et al.*, 1998;Feldman *et al.*, 2000) and homologous with amino acid transporters belonging to the solute carrier 6 (SLC6) gene family.

The functional role of an highly conserved sequence, consisting of three consecutive glycines (Gly85-Gly86-Gly87), has been investigated by alanine scanning mutagenesis; this sequence is located in the first extracellular loop of the protein, close to Arginine 76, the residue that participates to the external gate of the protein.

The functional characteristics, i.e. transport activity, apparent affinity, interaction with different cations, were derived from electrophysiological measurements (TEVC, Two Electrode Voltage Clamp), and uptake experiments. Additional informations about the correct targeting to the plasma membrane of the glycine mutants have been obtained performing optical measurement of the surface expression by the single oocyte chemiluminescence (SOC) technique pioneered by Zerangue (Zerangue *et al.*, 1999) and used by others (Haerteis *et al.*, 2009;Bossi *et al.*, 2011).

Changes in the transport mechanisms observed for many of the analyzed mutants, indicated a relevant role of the glycine triplet in the transport function, that it was confirmed by the alterations of the uncoupled currents and the apparent affinity.

The second part of my PhD work, covered the analysis of the relationship between temperature and substrate affinity in the ion-coupled cotransporter KAAT1 (from a poikilotherm invertebrate) in comparison with rGAT1, the GABA neuronal transporter originating from a mammalian (homeotherm) animal. Observations based on the rate of

transport, and the effects on the presteady-state currents, i.e. the electrical signal arising from the initial steps of the transport cycle (Parent *et al.*, 1992;Parent *et al.*, 1992;Mager *et al.*, 1998;Bossi *et al.*, 1999a) were studied in order to evaluate the kinetic properties of the cotransport system at more physiological temperatures. A strong increase of transmembrane currents was measured in both transporters at higher temperature (30°C); the increased maximal transport-associated current (I_{max}) was counterbalanced by a lower apparent substrate affinity (K_{05}). The inverse relationship between affinity and current supports previous observations in the intestinal tranporter PepT1(Bossi *et al.*, 2012).

Contents

Chapter 1

Introduction

1.1 Plasma Membrane Transport

For the life of the cell the provision of energy and nutrients is fundamental; efflux and influx of different substances such us amino acids, sugars, nucleotides and inorganic ions are necessary to maintain their biological activities.

The plasma membrane is an essential component of all the cells of the organism; it acts as a barrier maintaining the intracellular environment separated from the outside and is selectively permeable to ions and organic molecules. The cell membrane consists of a lipid bilayer containing many integral proteins bounded by electrostatic interactions. These proteins exert the function of transport, enzymatic activity, signal transduction, cell-cell recognition, attachment to the extracellular matrix and the cytoskeleton.

Transport processes are the basis of the cell physiology and fundamental for survival; they involve carrier proteins that play an important role in the cell physiology; transport proteins are present in virtually every cell and are essential for life of all prokaryotic and eukaryotic organisms; they have different functional and structural properties and are divided in two groups: the solute carriers (SLC) and the others transport proteins (Fig.1.1). SLC transporters include more than 43 gene families coding for passive transporters, exchangers and co-transporters, that show a sequence identity at least of 20-25%.

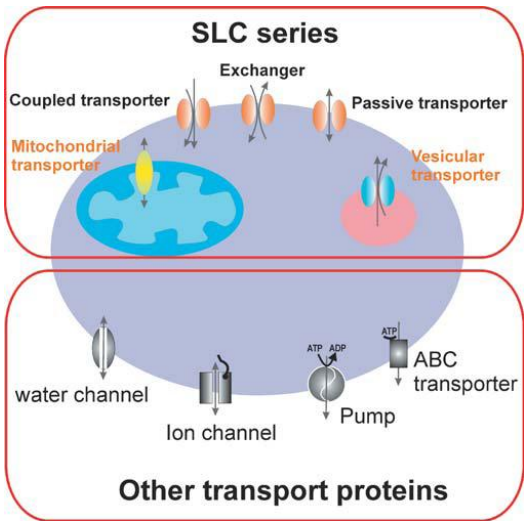

***Fig.1.1**: (SLC)- and non-SLC-transporters expressed in the plasma membrane or in intracellular compartment membranes. (Hediger et al., 2004).*

1.2 Neurotransmitter Transporters

Communication between neurons is achieved through release of polytopic glycosilated proteins, called neurotransmitters, that use ionic electrochemical gradients to drive the transport of substrate with hight affinity (in a range from 1 to 10 μM) with a mechanism that in most cases is a cotransport. Based on their molecular structure, on the distribution and on the transported ion, they have been classified (Hediger *et al.*, 2004). Vescicular transporters move neurotransmitters into synaptic vescicles regulating the concentrations of substances within them; they utilize on a proton gradient created by the hydrolysis of adenosine triphosphate (ATP) in order to carry out their work: vescicle ATPase hydrolyzes ATP, causing protons to be pumped into the synaptic vescicles and creating a proton gradient. Then the efflux of protons from the vescicle provides the energy to bring the neurotransmitter into the vesicle.

For the biogenic amines, synaptic transmission is terminated by integral membrane proteins, called neurotransmitter transporters, located on the pre-synaptic terminal. They are divided in two major families: Na^+/K^+ -dependent transporters (SLC1), responsible of the uptake of excitatory aminoacids as aspartate and glutamate (Kanai & Hediger, 2004); Na^+/Cl^- -dependent transporters (SLC6), as the GABA, serotonin and catecolamine transporters (Chen *et al.*, 2004a). These transporters utilize the asymmetric distribution of Na^+ and Cl^- across the plasma membrane to catalyze the thermodynamically unfavorable movement of neurotransmitter back into the pre-synaptic neuron for replenishment of neurotransmitter stores and subsequent neural firing. As the transport of substrate is coupled to ion transport (symport), these secondary active transporters are known as neurotransmitter sodium symporters (NSS). Dysfunction of NSS leads to a variety of disorders such as orthostatic intolerance and depression. Not surprisingly, these proteins are the primary pharmacological targets of antidepressants such as fluoxetine (Prozac) which is specific for the serotonin transporter. Furthermore, studies have shown that these transporters directly interact with drugs of abuse, cocaine and amphetamine.

1.2.1 NA^+/CL^- dependent neurotransmitter transporter family SLC6

The SLC6 family is among the largest SLC families, containing 20 genes that encode a group of highly similar transporter proteins (Table 1). They are secondary active transporters performing transport of amino acids and amino acid derivatives into cells, using, as mentioned in the previous paragraph, cotransport of extracellular Na^+ as a driving force for substrate translocation against chemical gradients (Chen *et al.*, 2004a) (Broer, 2006;Hoglund *et al.*, 2005). In addition, the SLC6 transporters are further classified as symporters, in that the coupled transport of Na^+ is performed in the same direction as substrate transport, although a few members also exhibit antiport activity by performing coupled-transport of K^+ (Rudnick & Clark, 1993) like for example, a subfamily of SLC6, called NATs (Nutrient Amino Acid Transporters),whom details are explained in the next paragraphs.

SLC1	The high affinity glutamate and neutral amino acid transporter family	7
SLC2	The facilitative GLUT transporter family	14
SLC3	The heavy subunits of the heteromeric amino acid transporters	2
SLC4	The bicarbonate transporter family	11
SLC5	The sodium glucose cotransporter family	12
SLC6	The sodium - and chloride - dependent neurotransmitter transporter family	20
SLC7	The cationic amino acid transporter/glycoprotein-associated family	14
SLC8	The Na^+/Ca^{2+} exchanger family	3
SLC9	The Na^+/H^+ exchanger family	11
SLC10	The sodium bile salt cotransporter family	6
SLC11	The proton coupled metal ion transporter family	2
SLC12	The electroneutral cation-Cl cotransporter family	9
SLC13	The human Na^+-sulfate/carboxylate cotransporter family	5
SLC14	The urea transporter family	2
SLC15	The proton oligopeptide cotransporter family	4
SLC16	The monocarboxylate transporter family	14
SLC17	The vesicular glutamate transporter family	8
SLC18	The vesicular amine transporter family	3
SLC19	The folate/thiamine transporter family	3
SLC20	The type III Na^+- phosphate cotransporter family	2
SLC21	The organic anion transporting family	20
SLC22	The organic cation/anion/zwitterion transporter family	18
SLC23	The Na^+-dependent ascorbic acid transporter family	4
SLC24	The $Na^+/(Ca^{2+}$-$K^+)$ exchanger family	6
SLC25	The mitochondrial carrier family	46
SLC26	The multifunctional anion exchanger family	11
SLC27	The fatty acid transport protein family	6
SLC28	The Na^+ - coupled nucleoside transport family	3
SLC29	The facilitative nucleoside transporter family	4
SLC30	The zinc efflux family	10
SLC31	The copper transporter family	2
SLC32	The vesicular inhibitory amino acid transporter family	1
SLC33	The Acetyl-CoA transporter family	1
SLC34	The type II Na+ - phosphate cotransporter family	3
SLC35	The nucleoside-sugar transporter family	23
SLC36	The proton-coupled amino acid transporter family	4
SLC37	The sugar-phosphate/phosphate exchanger family	4
SLC38	The System A & N, sodium-coupled neutral amino acid transporter family	6
SLC39	The metal ion transporter family	14
SLC40	The basolateral iron transporter family	1
SLC41	The MgtE-like magnesium transporter family	3
SLC42	The Rh ammonium transporter family (pending)	3
SLC43	Na^+-independent, system-L like amino acid transporter family	3
SLC44	Choline-like transporter family	5
SLC45	Putative sugar transporter family	4
SLC46	Heme transporter family	3

***Table 1**: List of the proteins of the „solut carriers" SLC family reporterd by "Human Genome Organisation"* – http://www.bioparadigms.org/slc/menu.asp.

Members of SLC6 family reside in the plasma membrane of neurons, glia and other cell types, such as platelets, must cells and basophils. They have also been found in tissues such as kidney, liver, placenta, adrenal medulla and the majority of them has a well defined biological function and physiological role, including known endogenous substrates, and is

divided into four subclasses on the basis of sequence similarity and substrate specificity (Broer, 2006)(Fig.1.2). Because the NSS genes were among the founding gene members of the SLC6 gene family, alternate designations for the family are often used, such as the "neurotransmitter sodium symporters," the "sodium-neurotransmitter symporter family," or the "Na^+/Cl^- -neurotransmitter transporter" family (Nelson, 1998;Beuming *et al.*, 2006).

The first cloned molecule in this family was the neuronal γ-aminobutyric acid (GABA) transporter, GAT1(Guastella *et al.*, 1990) and cloning proceeded rapidly to more than a dozen known sequences, some of them named according to their primary endogenous transmitter such as transporters for norepinephrine (NET), serotonin (SERT), dopamine (DAT), glycine (GLyT), and taurine (TauT). In 1992, Handler and coworkers reported the isolation of the canine betaine transporter (BGT-1) cDNA, which was obtained by expression cloning in oocytes from a size-fractionated cDNA library constructed from MDCK cells maintained in hypertonic medium; mRNA from MDCK cells maintained in hy-pertonic medium showed increased induction of betaine uptake in oocytes (Matskevitch *et al.*, 1999). Different strategies based on homology with these previous and the on-coming cDNA sequences from different cDNA sources resulted in the cloning of the rest of transporters of this superfamily, whom members share the 40-60% amino acid sequence homology. Homologous transporters have been identified in insects, worms, and yeast.

The sequence analysis combined with biochemical approaches suggested a membrane topology with 12 putative transmembrane (TM) helices with intracellular N- and C-termini and a large glycosylated loop between transmembrane helices III and IV (Fig.1.3) This membrane topology has been experimentally verified across the monoamine (Torres *et al.*, 2003), GABA (Kanner, 2006) and glycine transporter subfamilies by a large number of studies, mainly using specific antibodies (Chen *et al.*, 1997;Navedo *et al.*, 2008) or site-selective biochemical labeling of Lys and/or Cys residues.

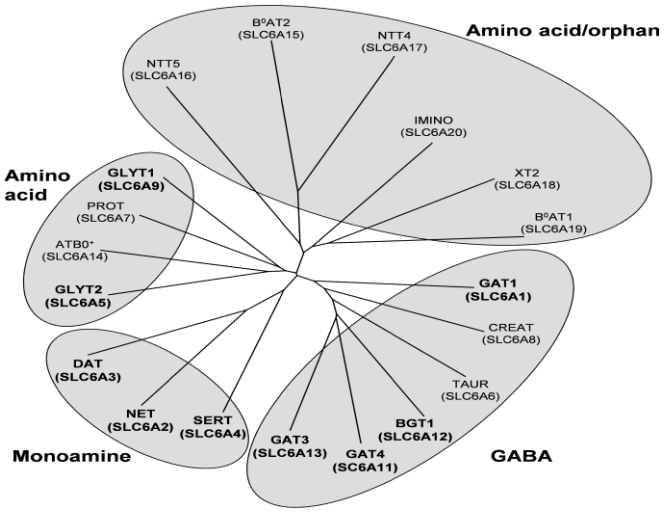

***Fig.1.2**: Phylogenetic tree of the SLC6 transporter family. NSS are found in fours subfamilies and are highlighted in bold (Kristensen et al., 2011).*

Another structural feature of this transporters family is a pair of Cys residues in extracellular loop 2 that form an intraloop disulfide bridge. The loop also contains sites for N-linked glycosylation (Olivares *et al.*, 1997). In the decade after the cloning of the NSS, substantial efforts were made to identify and characterize the regions and specific residues that contribute to core transporter functions such as substrate binding and translocation. SCAM (substituted cysteine accessibility) analysis of the GABA and glycine transporters has been carried out to a lesser extent, although several key residues for transporter function of GAT1 have been identified by mutagenesis studies (Bismuth *et al.*, 1997;Kanner *et al.*, 1994;Keshet *et al.*, 1995;Mager *et al.*, 1996;Zomot & Kanner, 2003).

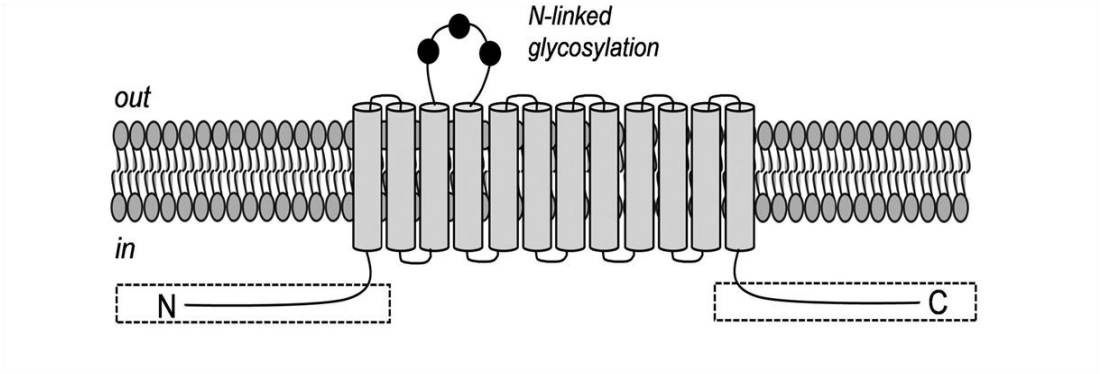

Fig.1.3*: Membrane topology of SLC6 NTTs*
(Kristensen et al., 2011).

This initial topology derived from bioinformatic approach has been confirmed through the first crystal structure, obtained by (Yamashita *et al.*, 2005) whose details are described in the next paragraph. LeuT structures have been established as valid templates for molecular modeling of the mammalian NSS, and LeuT is emerging as an important model protein for biophysical and computational studies addressing the molecular dynamics underlying NSS function and pharmacology (Caplan *et al.*, 2008;Celik *et al.*, 2008).

1.2.2 Functional and pathological role

As all the SLC6 transporters are expressed in the central nervous system (CNS), their primary physiological role is the regulation of neurotransmitter homeostasis. However, some of them are also found in other tissues (see *paragr. 1.3*), where they serve important physiological functions. Their central role is to mediate the rapid uptake from the extracellular space of synaptically released neurotransmitter within and around synapses. The uptake can be maintained against very large concentration gradients and the kinetics of NSS-mediated transport follows the Michaelis- Menten model with substrate K_M values in the lower micromolar range and maximal turnover rates ranging from 1 to 20 substrate molecules per second. The relationship between extracellular concentrations of Na^+ and Cl^- and transport activity also follows Michaelis-Menten kinetics with K_M values in 5 to 50 mM range (Kristensen *et al.*, 2011).

Fours of nine SLC6 transporters represent important drug targets for treatment of a broad array of brain diseases in clinical use. For example, GABA transporters are involved in seizures and are target of anticonvulsants; serotonin (SERT), dopamine (DAT) and noreprinefine (NET) transporters are targets of antidepressants and psychoactive substances of abuse such as amphetamine, 3,4-metilen-diossi-metamfetamine (MDMA or ectasy) and cocaine. Dysfunctions that involve neurotransporters include Parkinson disease, epilepsy, autism, startle disease atc (Table 2).

The SLC6 transporters

Human Gene	UniProt Name[a]	Endogenous Substrate	Tissue Distribution	Link to Disease
*SLC6*A1	GAT1	GABA	Brain, peripheral nervous system	Epilepsy, schizophrenia, anxiety
*SLC6*A2	NET	Norepinephrine	Brain, peripheral nervous system, adrenal gland, placenta	Depression, orthostatic intolerance, anorexia nervosa, cardiovascular diseases
*SLC6*A3	DAT	Dopamine	Brain	Parkinson's disease, Tourette syndrome, ADHD, addiction
*SLC6*A4	SERT	Serotonin	Brain, peripheral nervous system, placenta, epithelium, platelets	Anxiety, depression, autism, gastrointestinal disorders, premature ejaculation, obesity
*SLC6*A5	GLYT2	Glycine	Brain, spinal cord	Pain, spasticity
*SLC6*A6	TAUT	Taurine	Brain, retina, liver, kidney, heart, spleen, pancreas	Taurine deficiency diseases, retinal blindness, abnormal renal development
*SLC6*A7	PROT	Proline	Brain	
*SLC6*A8	CT1	Creatine	Ubiquitous	Creatine deficiency syndrome, mental retardation, musculoskeletal disorders, cardiomyopathy
*SLC6*A9	GLYT1	Glycine	Brain, pancreas, uterus, stomach, spleen, liver, retina	Schizophrenia
*SLC6*A10[b]				
*SLC6*A11	GAT3	GABA	Brain	Epilepsy
*SLC6*A12	BGT1	Betaine, GABA	Brain, kidney	Epilepsy
*SLC6*A13	GAT2	GABA	Brain, liver, kidney	Epilepsy
*SLC6*A14	ATB0+	Neutral, cationic amino acids	Lung, trachea, salivary gland, mammary gland, stomach, pituitary gland	
*SLC6*A15	NTT73	Large neutral amino acids	Brain	
*SLC6*A16	NTT5	Unknown	Testis, pancreas, prostate	
*SLC6*A17	NTT4	Neutral amino acids	Brain	
*SLC6*A18	B0AT3	Neutral amino acids	Kidney	
*SLC6*A19	B0AT1	Neutral amino acids	Intestine	Hartnup disorder
*SLC6*A20	XTRP3	Proline, pipecolate, sarcosine	Brain, kidney, small intestine, thymus, spleen, ovary, lung	

***Table 2**: List of SLC6 transporters: Link to Disease.*

1.3 …..a structural template for understanding fundamental aspects of SLC6 NSS function….

It is important to remind that before the determination of the first high-resolution X-ray crystal structure of a bacterial homolog to the mammalian *SLC6* transporters, the structural understanding of *SLC6*- NSS was based on indirect observations derived from extensive biochemical and mutagenesis studies that provided indispensable insight into transporter topology and secondary structure but

limited information on the tertiary structure. This was revised in 2005, when Yamashita et collaborators reported an high-resolution X-ray crystallographic structure of a prokaryotic homolog to the *SLC6* transporters, the leucine transporter (LeuT) from the thermophile bacterium *Aquifex aeolicus* (Deckert, *et al.* 1998).

Although LeuT is evolutionary distant from the *SLC6* NSS (20–25% overall sequence identity), the protein has proved to be a suitable and highly useful structural and functional template for the *SLC6* NSS (Singh *et al.*, 2007).

1.3.1 Structure of LeuT, a bacterial Na^+/Cl^- dependent transporters homologue

The structure of LeuT confirmed many predictions made for *SLC6* transporter architecture by revealing 12 transmembrane (TM) regions connected by short intra- and extracellular loops with intracellular N and C termini (Fig.1.4); all the TMs are almost exclusively α-helical, except short unwound segments in TM1 and TM6. Several α-helical elements are also present in the intra- and extracellular loops. The TMs pack as an intertwined helical bundle into a cylindrical shape that can be divided into an interior and outer part; the substrate binding site is located at the core of the transporter. The inner ring is formed almost exclusively by TM1, TM3, TM6, and TM8 and holds a central substrate binding site in which the substrate (Leu) and two Na^+ ions are accommodated. In all substrate-bound LeuT structures, this central substrate binding pocket is occluded from both the external and internal medium (Singh *et al.*, 2007;Singh, 2008;Yamashita *et al.*, 2005;Zhou *et al.*, 2007).

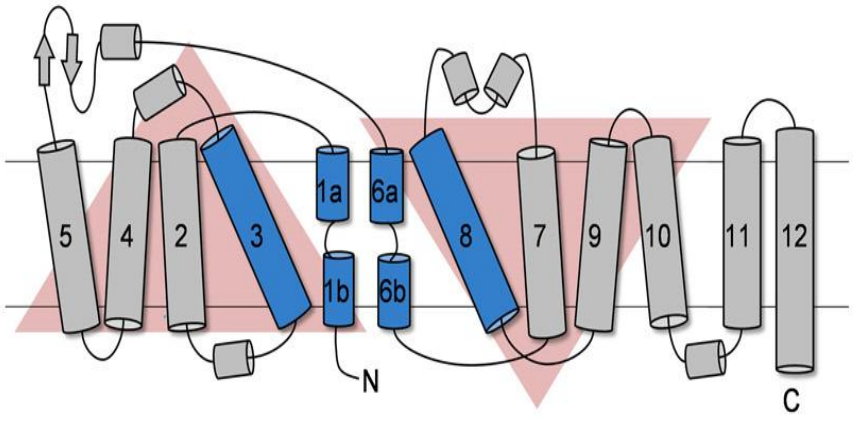

***Fig.1.4**: Topology of LeuT, a bacterial homolog of SLC6 NTTs (Kristensen et al, 2011).*

Near this unwound region excepted from TM1 and TM6, that takes part in the substrate and ions binding, the segments 3 and 8 are rich in conserved amino acids compared to the other members of SLC6 family. These residues have a relevant role in the interaction with the substrate and ions. In the Figure 1.5 the parts of the protein in the unwound region are visible. In particular, the binding pocket is mostly formed by main-chain atoms of these regions interacting with the α-amino and α-carboxy groups of leucine.

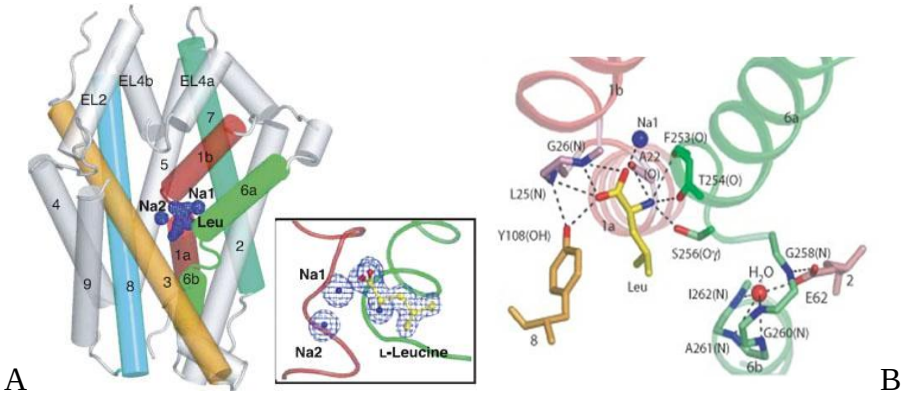

A B

Fig 1.5*: Leucine binding site: A: The insert shows the electron density of the substrate leucine and of the two sodium ions (Na1, Na2) between the unwound TM1b (in red) and TM6a (in green). B: In a larger view the interaction between the hydrogens bond (dashed lines) and ionic interaction are highlighted.*

In the crystal structure, the L-leucine substrate appears to be found as a zwitterions, the binding site is completely dehydrated and specifically, the negatively charged carboxy group of the leucine is near the positively charged end of the TM1b helix dipole, while the positively charged amino group of leucine is very close to the negatively charged residues on TM1a and on the TM6a helix dipole. In the Fig.1.5B, the exact hydrogen bond are shown: the carboxy group interacts with a sodium ion, amide nitrogens from Leu 25 and Gly 26 in TM1, and a hydroxyl from Tyr 108 in TM3. Subsequent work showed TM1 and TM3 are involved in the traslocation pathway (Kanner, 2003;Melamed & Kanner, 2004;Zhou *et al.*, 2004;Zhou & Kanner, 2005). Particularly interesting is Tyrosine 108 in TM3, because it makes contact with the substrate and also forms an hydrogen bond with Leu25, stabilizing in this way the irregular structure near the unwounded region of TM1;

other important residues are Glu 62 which stabilizes the unwound region of TM6, and Ser256 which is responsible for stabilizing the amino group of the leucine, and which is also conserved in the eukaryotic homologue (the amino acid transporter KAAT1 from *Manduca sexta*) that can transport the same substrate and the details will be better discussed in the next paragraphs. The described binding sites, when compared to sequence information of mammalian transporters, allow to infer some conclusions about the selectivity shown by the euckariotic homologues. In fact, biogenic amine transporters NET, DAT and SERT, in the corresponding position of Gly 24, have an aspartate, which substitutes the carboxy group of the substrate (leucine for $LeuT_{Aa}$, GABA for GATs and Glycine for GlyTs) and coordinates with sodium.

The exceptionally high resolution of the present structure indicates with very high probability the localization of the two sodium ions (named N1 and N2), binding pocket (Fig.1.6).

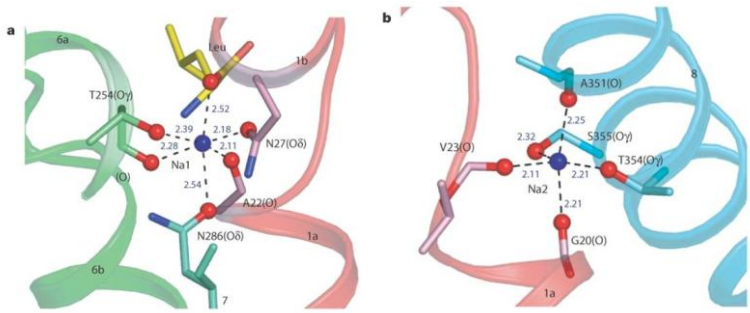

***Fig. 1.6**: Sodium ion binding sites (Yamashita et al., 2005).*

They are located halfway across the membrane bilayer within 6 A° of the α- carbon of the bound substrate molecule. The Na1 pocket is determinate from the following residues: Ala22 and Asn27 from the TM1, Thr254 from TM6 and Asn286 from the TM7. The Na2 binding site is positioned between TMs 1 and 8 and makes direct contact with Gly 20 and Val 23 (TM1) and Ala351, Thr 354 and Ser355 in the TM8 (as shown in Fig 1.6, *panel b)* These ions have a key role in stabilizing the binding of the L-leucine substrate and also the core of the protein. Na1, making contact with leucine (as mentioned above) may imply a strict coupling in the transport, indicating that probably the first event in the transport activity is the binding of ions inside the transporter and that substrate binding is possible

only after conformational change. Analyzing the sequences of the mammalian transporters, it is evident that Na1 site is conserved while N2 site appears less conserved, supporting the difference in the stoichiometry of the different transporters.

As the nomenclature describes, the function of these transporters that belong to the SLC6 family is dependent on Na^+ and in many instances also on Cl^- as cotransported ion, that may have the role of stabilizing the identified external gate, supporting some considerations made on chloride and its role in the functioning of the mammalian transporters. In two papers (Singh *et al.*, 2007;Zhou *et al.*, 2007), it has been shown the crystal structure of LeuT with one molecule of a tricyclic antidepressant (TCA) bound. In many respect, the structure agrees with and extends the biochemical data on transporters of the NSS family, even if some differences exist in the structure and function of the two transporters. For example, the neurotransporters require chloride for transport, while prokaryotic transporters do not. The majority of mammalian SLC6 transporters, including all nine members of the NSS subfamily are functionally dependent on extracellular Cl^-. In contrast, the function of prokaryotic SLC6 homologs, including LeuT, is Cl^--independent (Kanner & Zomot, 2008;Zhao *et al.*, 2010;Zomot *et al.*, 2007). It is remarkable that the negatively charged residue is conserved in the prokaryotic transporters but not in the mammalian transporters (Zomot *et al.*, 2007;Forrest *et al.*, 2007); structural analysis of LeuT-based homology models of GAT1 and SERT with Cl^- docked into the equivalent position of Glu290 in LeuT showed that this could accommodate Cl^- by coordination to the amide group of Gln291 and the hydroxyl groups of Ser331, Ser295, and Tyr86 (human GAT1 numbering). Accommodated at this site, Cl- is close to Na^+ in the Na1 site, thus supporting the idea that Cl^- is translocated along with Na^+ and substrate during transport {2041}. Recent studies of measurements of currents associated with conformational changes in DAT to study the kinetics of the transport mechanism found that increasing intracellular Cl^- concentration, thus saturating DAT with Cl- during the return step, facilitated transporter turnover, suggesting a variable functional role of Cl- among the SCL6 NSS, which highlights the presently poorly understood role of Cl^- for the transport function (Oliveria *et al.*, 2007).

The organization in complex quaternary structures has been hypothesized for the NSS transporters: LeuTAa forms a dimer in the crystal (Yamashita *et al.*, 2005).

1.4 Electrophysiological properties

In general, neurotransmitter transporters have lower turnover rates when compared to ion channels (10^2- 10^4 s^{-1} *vs.* 10^6-10^7 s^{-1}): this feature prevents accurate electrophysiological investigations in native tissue. Since the cloning of these transporters and their expression in heterologous system, macroscopic currents can be measured with electrophysiological techniques, for nearly all transporters. The most powerful electrophysiological method is the "voltage –clamp" technique because of its several advantages over other techniques used in transport studies, as i) the membrane voltage of the cell is under control; ii) the temporal resolution is high; iii) the data are immediately available to be analyzed and interpreted. More details of the two electrode voltage-clamped (TEVC) technique, that it has been used to perform the experiments in this thesis, is given in the *Method* section.

The transporters of the SLC6 family usually display three kinds of voltage dependent currents: "transport-associated current", a coupled-current (I_{tr}) associated to the translocation of the substrate; "presteady-state" current" (I_{pre}), a transient current; uncoupled or "leakage" current.

The first one, I_{tr} is due to the movement of the ion across the membrane when a specific substrate is added to the solution. It depends on membrane potential, concentration of substrate and on the presence of the driver ions and it represents a good tool for the functional study of a protein. Recordings of these currents were performed in the past in our laboratory, in non injected and KAAT1 (insect amino acid transporter) -injetcted oocytes, at fixed membrane potential (-80 mV) or using a voltage pulse protocol indicated in the Fig.1.7. It was evident to observe a different behavior of the control oocytes respect to the injected ones: addition of the substrate leucine 1mM to the KAAT1-expressing oocytes produced an increase on the transport-associated currents.

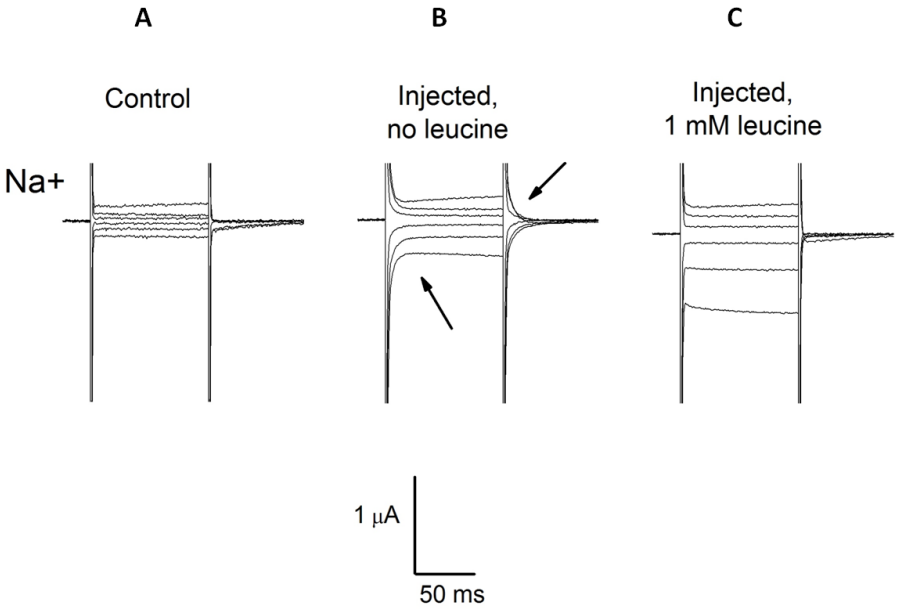

Fig1.7.: *Voltage-dependent currents in control and KAAT-1 expressing oocytes. Recordings of membrane currents elicited by voltage steps to –160, –120, –40, 0, and +40 mV (from V h =–80 mV) in a control oocyte (A) and in a KAAT1-expressing oocyte, before (B) and after the addition (C) of 1mM leucine in the presence of Na^+ ion.*

Transport-associated current may be used in determining the *I/V* relationship and the apparent affinity of the transporter for the organic substrate varying the concentration of the substrate while keeping constant the ionic composition of the solution. In section *Result, Chapter 3,* these properties of KAAT1 cotransporter will be reported, as well as the apparent affinity for the Na^+ driving ion that, it can be determined isolating the transport-associated current elicited by application of a fixed substrate concentration in the presence of different Na^+ concentrations.

The I_{pre} is observed in the absence of organic substrate and is typical of most of the cloned SLC transporters (Bossi *et al.*, 1998;Hazama *et al.*, 1997;Lester *et al.*, 1996). It derives from the movement of intramembrane charges induced by rapid changes of voltage or substrate concentration (Mager *et al.*, 1993) and it may due to the movement of ions inside the protein or the movements of intrinsic charges of the transporter itself (Peres *et al.*, 2004). This transient current appears to be a relevant distinctive feature of the transporter proteins and an important clue to understand their function. In the Fig.1.7, the arrows show

the transient current elicited by different voltage steps, in KAAT1-expressing oocytes, in the presence of Na^+ ion.

Finally, the "leakage" current arises from condition in which the transporters can allow the occasional translocation of ions even when the substrate is not present (Lester *et al.*, 1996). It is elicited by the presence of the substrate and it is believed to be stoichiometrically coupled to the movement of substrate, in particular, the charge that shifts across the cell membrane through one transport cycle varies from zero (when the net flow of charge is zero, for example in the case of SERT) to a maximum of 2 charges (for example the isoform GlyT2A of the glycine transporter).

A peculiar feature of the uncoupled current is its enhancement in lithium and this characteristics allow to distinguish transporters from channels, in which Li^+ cannot generally replace Na^+. An example is shown in the Fig.1.8., reported below.

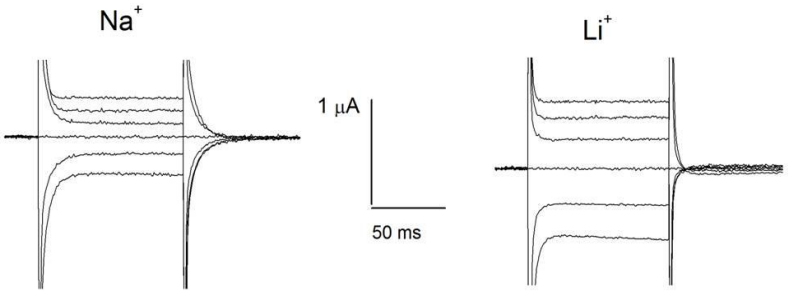

Fig.1.8: *Representative current traces in response to 200-ms voltage jumps from -160 to 0 m V (Vh= -60 m V) in solutions containing the indicated cation for wt KAAT1.*

1.5 Transport Mechanism

The electrophysiological properties of transporters together with information derived from flux rates measurements and other techniques were used to give hypothetical descriptions of the transport mechanism and to propose different kinetic models. Since discovery of NSS transporters various theoretical transport mechanisms have been proposed and the "alternate access model" is the widely accepted model. The movement across the membrane is guaranteed by an extracellular hydrophilic cavity between the compartment

and either side of the membrane in which the binding site for the substrate is located. After the substrate is bound, the closing of the external gate and the opening of the internal one allows the molecule to enter in the cytoplasm (Fig.1.9). The transporter can now go back to the initial conformation and interact with a new molecule of substrate. For ion-coupled transporters such as the SLC6 NSS, the conformational equilibrium between "inward"- and "outward"-facing states is determined by binding of ions and substrate. Although other models for this transport have been proposed (DeFelice *et al.*, 2001;Lester *et al.*, 1996), the alternating access model form the model for the majority of current efforts directed toward establishing the structural mechanisms of transport.

The increasing number of structures of prokaryotic transporters sharing the LeuT 5+5 inverted repeat fold is emerging as a very useful platform for elucidating the structural basis for NSS transport. Specifically, these structures provide "snapshots of different transporter conformations, captured along what seems to be a transport cycle consistent with an alternating access mechanism.

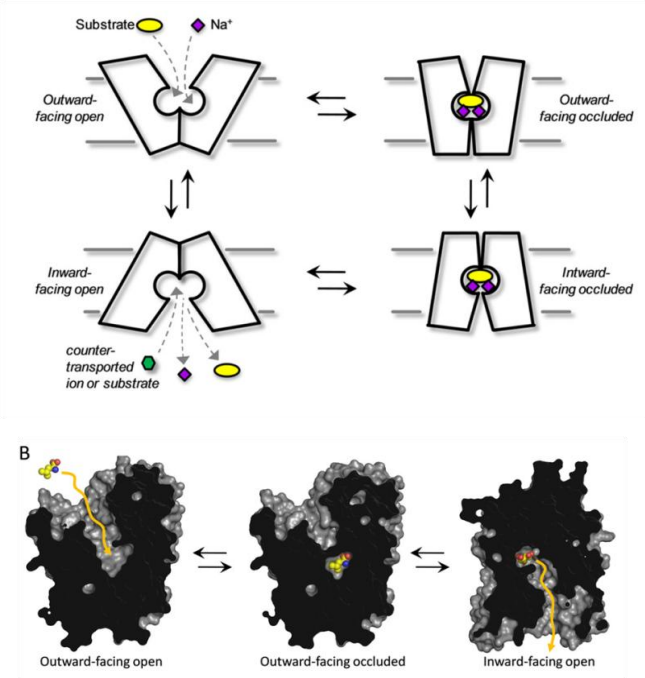

***Fig.1.9**: Alternating access mechanism and gating regions. A, schematic representation of the conformational states the transporters have to shuttle between to move substrate from the extracellular space to the cytoplasm. B, cross-sectional illustrations of transporters with a 5+5 internal repeat motif crystallized in distinct conformations corresponding to different states in the alternating access mechanism (Kristensen et al., 2011).*

The fact that transporters sharing the 5+5 internal repeated fold also share a general transport mechanism allows to use it as template for the development of models of the molecular events underlying transport in the *SLC6* NTTs (Abramson & Wright, 2009;Gouaux & MacKinnon, 2005).

Many other studies have demonstrated that transport- associated conformational changes in *SLC6* NSS are consistent with predictions from alternating access models; these include the use of voltage-clamp fluorometry to show movement of TM1 during transport (Meinild *et al.*, 2009) and SCAM analysis to confirm that TM8 lines the intracellular pathway of GAT1 (Ben Yona & Kanner, 2009). Furthermore, SCAM analysis of TM5 in SERT shows that the intracellular region of this domain becomes exposed to the intracellular side when SERT is locked in an inward-facing conformation (Forrest *et al.*, 2008), using SERT as a model protein for SCAM experiments to validate the principle motions of the "rocking bundle" model.

1.6 Nutrient Amino Acid Trasporters (NATs)

As just mentioned above, in addition to neurotransmitter transporters, the NSS family also comprises transporters for nutrients, in particular for amino acids, that play fundamental roles in several cellular functions including protein synthesis, hormone metabolism, catalytic functions, nerve transmission, regulation of cell growth, production of metabolic energy, synthesis of purines and pyrimidines, nitrogen metabolism and biosynthesis of urea. Molecular mechanisms of accumulation and redistribution of essential amino acids are poorly understood in mammals and virtually unknown in other organisms, including insects.

A variety of amino acid transporters with overlapping substrate specificities ensure an adequate supply of these important solutes, reviewed in (Palacin *et al.*, 1998) and a subgroup of the NSS family comprising nutrient amino acid transporters (NATs) has been identified (Boudko *et al.*, 2005). To this new group belongs KAAT1 (K^+ -coupled Amino Acid Transporter), an invertebrate neutral aminoacid transporter cloned from the midgut of the larva of the lepidoptera *Manduca sexta* (Castagna *et al.*, 1998;Feldman *et al.*, 2000). The role of insect NATs in the uptake and redistribution of essential amino acids is strongly supported by the functional consensus of the five cloned and characterized

transporters (Fig.1.10) underlined members of insect NATs, namely A. aegypti aeAAT1, M. sexta KAAT1 and CAATCH1, and Anopheles gambiae proteins agNAT8 and agNAT6; NATs plasticity and NSS conservation are essential in evolution and imply different selection mechanisms (Montell *et al.*, 2002): the second group could be stabilized by adaptation to particular substrates (neurotransmitters) and electrochemical homeostasis of the neuronal environment. According to (Boudko *et al.*, 2005) the plasticity of NAT phenotypes may include tuning of electrochemical properties, substrate affinity, and selectivity of NATs in different species.

1.6.1 NATs in the Mammals

The amino acid transporters analyzed by sequence homology fall into the following five families: the Na^+/Cl^- -coupled neurotransmitter/amino acid transporter family (SLC6), above reported; the EAAT/ASCT transporter family (SLC1); the CAT transporter family (SLC7); the 4F2heavy chain/light chain and rBATheavy chain/light chain transporter family (SLC3+SLC7); the ATA/SN family of AAAP-related transporters (amino acid and auxin permeases, SLC38); the TAT transporter related to the monocarboxylate transporter family (MCT, SLC16) (Zhang *et al.*, 2008). Antiport is the prevalent kind of amino acid transport in mammalian tissues and this reflects the fact that most tissues or cells have excessive amounts of non essential amino acids but may lack essential ones. Almost any cell can synthesize alanine, glutamine, glutamate, asparagine and aspartate from metabolic intermediates, whereas branched-chain amino acids, aromatic amino acids and most cationic amino acids are essential. Antiporters amino acid transporters are very important for vectorial transport across epithelia but transport mechanisms are not well conserved within families (Palacin *et al.*, 1998).

For example, it has been shown that neuronal and glial glycine transporters have different stoichiometries: the neuronal GlyT2a transported two net charges per glycine, whereas a transfer of only one net charge was observed in the glial GlyT1b. Both transporters depended on the presence of chloride and a cotransport of 1 mol 36 Cl per mol of substrate was demonstrated in both cases (Dodge & Scott, 2000). The Na^+-cotransport stoichiometry is not the only mechanistic parameter that varies in this family. GlyT1b and GlyT2a

mediate the cotransport of chloride, whereas an exchange of chloride ions was observed in the case of the GABA transporter GAT-1 (Hennigan *et al.*, 1993a). Although transport depends on Cl^-, Cl^- doesn't contribute to the driving force of the transporter because it is exchanged. The $2Na^+$/1GABA cotransport is thus accompanied by the net transfer of two charges per cycle rather than one (Loo *et al.*, 2000).

The family of Na^+/Cl^--dependent amino acid transporters has evolved in a separate way in some insect species such as lepidoptera. In contrast to the Na^+ gradient that prevails in mammalian and other eukaryotic tissues, a K^+ gradient is exploited for intestinal reabsorption of amino acids in these insects (Castagna *et al.*, 1998;Miszner *et al.*, 2007;Caterina *et al.*, 1997). An excellent review by Kilberg's group (Malandro & Kilberg, 1996) describes the molecular biology of the amino acid transporters cloned in 1995. The molecular identification of amino acid transporters or related proteins leads to ongoing studies on the structure-function relationship and the molecular genetics of the pathology associated with these transporters.

Epithelial resorption of amino acids across the apical membrane in the kidney and intestine is thought to be carried out by four different transporters (Broer, 2008). Anionic amino acids are taken up by a Na^+-dependent aspartate/glutamate transporter, which has been designated system X^-AG . Molecular cloning has identified this transporter as EAAT3. Cationic amino acids are taken up by system $B^{0,+}$ the molecular correlate of this transporter being the heteromeric amino acid transporter rBAT/$B^{0,+}$ AT (Broer, 2009); proline and glycine are thought to be transported by the IMINO system (Broer *et al.*, 2004b).

The primary mediator for absorption of neutral and many essential amino acids across the apical membrane of the small intestine and kidney is the Na^+ -dependent transporter B^0AT1 [broad neutral (0) amino acid transporter 1; SLC6A19 (solute carrier family 6 member) (Castagna *et al.*, 2009). System B^0 has been characterized in jejunal brush border vesicles, bovine epithelial cells, and Caco-2 cells. Many studies suggest this system is a Na^+ -dependent, chloride-independent transporter that accepts a wide variety of neutral amino acids. Failures to resorb amino acids in the kidney and intestine underlie a number of inherited transporter diseases, with and mutations of system B^0 thought to cause Hartnup disorder, a symptomatically heterogeneous disease, largely limited to the kidneys and the small intestine and characterized by high levels of fecal amino acids and renal

aminoaciduria. Hartnup disorder has been a model disease because it illustrates the principles of amino acid resorption in epithelial cells.

1.6.2 NATs in the Insects

A phylogenomic analysis suggests that of 10 SLC families participating in mammalian amino acid transport, 9 are present in insect, two of which, SLC6 and SLC7, represent the major component of essential amino acid transport (Boudko, 2012). The subfamily, comprising NATs exist in Bacteria, Archea, Protozoa, Fungi ad Metozoa; other mammalian representatives of these clusters have been recently cloned and characterized (Broer *et al.*, 2004b;Broer, 2006;Verrey *et al.*, 2005). B^0 and IMINO system mentioned above include in the same cluster pairs of orthologous transporters found in insect genomes and defined as mammalian and insect NATs (Fig.1.10). B^0-like functionality was also reported earlier in two NATs cloned from Manduca sexta (Ms): KAAT1 (Castagna *et al.*, 1998) and CAATCH1 (Quick & Stevens, 2001). The caterpillar transporters form an insect-specific NAT cluster with 2–9 genes found in genomes of other insect species.

MsKAAT1 is the first characterized in the midgut of Manduca sexta NAT of the SLC6 family (Castagna *et al.*, 1998). Several NATs-SLC6 members, as AeAATI in mosquito B^0-like NAT and DmNAT1 in D. *melanogaster* have been characterized to explore mechanisms for the essential amino acid absorption in model dipteran insects. The identification and functional characterization of new B^0 -like and narrow specificity transporters of essential amino acids in fruit fly and mosquitoes leads to a fundamentally important insight: NATs act as the active core of a transport network that mediates active alimentary absorption and systemic distribution of essential amino acids.

The expression of all analyzed NATs in the posterior and anterior regions of the larval alimentary canal correlates with nutrient amino acid absorption (posterior midgut) and secretory functions (salivary gland and cardia). From the results of heterologous functional characterization, insect NATs represent normally rectifying (unidirectional) mechanisms that are predominantly driven by Na^+ motive force.

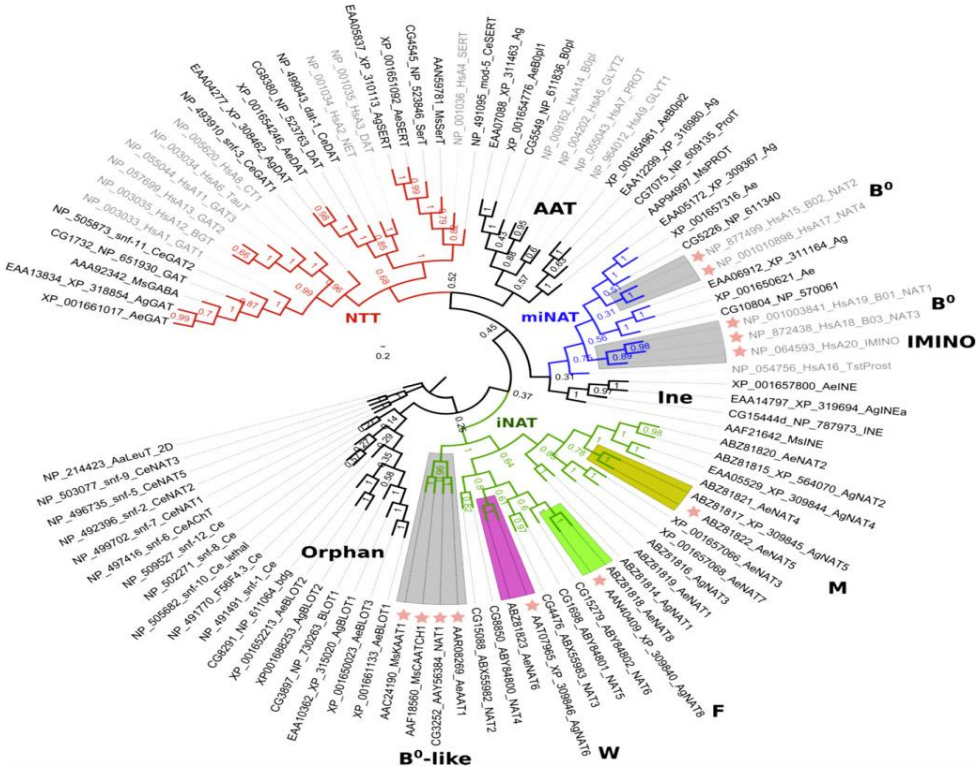

***Fig.1.10**: Phylogenomic tree of selected insect and mammalian SLC6 families (Boudko, 2012).*

Many insects NATs are also capable of using an inward K^+ motive force that may exist in specific conditions when high extracellular activity of K^+ ions and large negative transmembrane voltages reverse K^+ flux.

NATs, such as in the mammalian B^0ATs (Broer *et al.*, 2004a) and caterpillar KAAT1 (Castagna *et al.*, 1998), also reflect adaptations of these organisms to a high (in mammals) versus trace (in caterpillars) availability of Na^+ in the animals'diets. The availability of Na^+ and K^+ also varies over the life history of insects. Even high extracellular Cl^- concentrations facilitate the functions of some insect NATs.

The first structure of the first NAT from thermophilic bacterium *Aquifex aeolicus*, LeuT, revealed substrate and ion-binding sites in substrate occlusion and outside in open conformations. The canonical structure of SLC6 members, including 12 transmembrane domains, is illustated above in the Fig.1.3.

In summary, functionally explicit NATs and NSS provide a unique model for the study of the evolution and structural adaptation of membrane transport proteins. Essential and

lineage specific NATs appear to be better suited than the highly conserved NTTs as targets for selective and environmentally safe management of disease vector mosquitoes and agriculture pest insects (Boudko *et al.*, 2005).

1.7 KAAT1 (K^+-coupled Amino Acid Transporter1)

1.7.1 Lepidopteran Cotransporter

The amino acid transport in the insects has similarities and also differences with the mammalian systems. The principal difference depends on body fluids composition: in the invertebrate, the Na^+ concentration is very low and furthermore, in midgut cells the Na^+/K^+ ATPase, which in mammals maintains the sodium and potassium gradients across the membrane, is not detectable.

Despite its broad substrate spectrum, KAAT1 shows a notably different substrate selectivity and affinity profile vs. mammalian B^0. In fact, it can efficiently use the inward K^+ gradient in addition to the canonical Na^+ coupling of the mammalian B^0 system (Castagna *et al.*, 1998). The heterologously expressed KAAT1 mechanism has L-amino acid selectivity with approximately even transport capacity for absorption of L-enantiomers of F, L (K_m Leu = 123 lM) M and I (Castagna *et al.*, 1997). The absorptive epithelium of the tobacco hornworm *Manduca sexta* is mainly formed by two types of cells: columnar and globet cell (see in Fig.1.11).

Goblet cells express a H^+ -ATPase that generates a proton-motive force in the first place, which in turn is converted into a potassium electrochemical gradient by the action of a $K^+/2H^+$ antiporter. The potassium is thereby transported from the hemolymph into the lumen. The combined action of H^+-ATPase and K^+ n/2H +antiporter generates a large potassium electrochemical gradient with a transapical voltage of approximately -240 mV and an alkalinization of the intestinal lumen up to a pH value of about 10. This gradient is used to drive the uptake of amino acids by K^+ -amino acid symporters, which are allocated to columnar cells in the midgut.

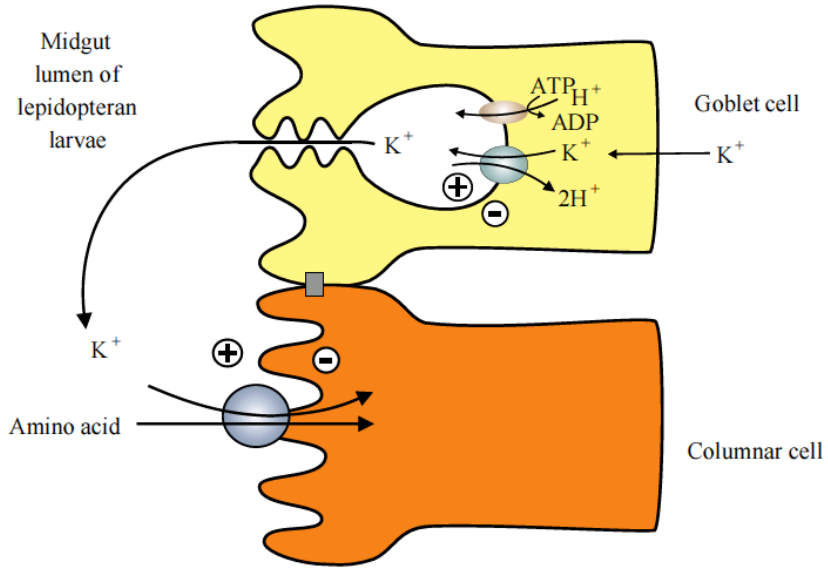

***Fig.1.11**: K + -coupled amino acid transporters in brushborder membranes of insect midgut columnar cells. The plasma membrane V-ATPase of goblet cells is an electrogenic proton pump which energizes electrogenic K + secretion via K + /2H + antiport (Castagna et al., 1997).*

Northern blot analysis and *in situ* hybridization probes showed that KAAT1 is specifically expressed with CAATCH1(Cation-anion Activated Amino acid Transporter/Channel) in the columnar cells (Castagna *et al.*, 1997;Feldman *et al.*, 2000). The K^+ -coupled uptake constitutes an important alternative to the strict Na^+ - dependence of known vertebrate transporters.

Potassium can be replaced also by other cations, such as Na^+ and Li^+, thereby demonstrating the relationship of KAAT1 to the Na^+ -dependent transporters of this family. In agreement with its similarity to the Na^+ and Cl^--dependent amino acid transporters, amino acid uptake via KAAT1 was also found to be chloride dependent. A cotransport stoichiometry of 2:1:1 (K^+ : Cl^- : amino acid) was proposed (Broer & Gether, 2012).

1.7.2 KAAT1

KAAT1 (K^+-coupled Amino Acid Transporter 1) is an invertebrate transporter for neutral amino acid cloned from the midgut of the larva of the lepidoptera *Manduca sexta* (Castagna *et al.*, 1998;Feldman *et al.*, 2000). KAAT1 cDNA contains 2882 bp with an ORF from nucleotides 103-2004 that encodes a 634-aa residue protein of 70 kDa. It shares the 38% of amino acid sequence with the neurotransmitters transporters, such as γ-aminobutyric acid (GABA) transporter, rat GAT1, and rat glycine transporter GLYT2 , as well the 37% identity to human brain specific L-proline transporter HPROT (Guastella *et al.*, 1990) (Fig.1.12).

***Fig.1.12**: KAAT1 alignment with sequences of members of the Na-Cl -dependent GABA transporter family: Putative transmembrane domains are underlined, and residues considered to be critical for function are highlighted by vertical arrows.*

As mentioned in the paragr. 1.3.1, this insect transporters belonging to NSS as KAAT1 show high sequence identity with the structural prototype of the family (LeuT). It is characterized by 12 TMs connected by short intra- and extracellular loops with intracellular N and C termini and it cointains two inverted repeats, with a central core that shows two broken α-helices where the substrate- binding residues are localized (Fig.1.4).

Furthermore, KAAT1 mediates the electrogenic uptake of neutral amino acids, showing a marked stereospecificity toward the L-isomers, except arginine and lysine; leucine, proline, threonine and methionine are all transported by KAAT1, as well other neutral aminoacids (Soragna *et al.*, 2004). The kinetics properties are similar to those of neutral amino acid transport systems in BBMV from this caterpillar (Caterina *et al.*, 1997). The cation dependency, amino acid uptake activity and kinetic properties of KAAT1 have subsequently been studied by many workers (Bossi *et al.*, 1999a;Bossi *et al.*, 2000;Castagna *et al.*, 2002;Liu *et al.*, 2003;Peres & Bossi, 2000;Vincenti *et al.*, 2000). Although KAAT1 utilizes K^+ as driver ion for the transport of amino acid, it can also mediate a Na^+ -coupled amino acid transport (and this ion can activate the amino acid transport even at low concentration) and Li^+ (Bossi *et al.*, 1999b;Castagna *et al.*, 1997;Hennigan *et al.*, 1993a). Kinetic studies conducted *in vitro* showed that the K_m for sodium is five times lower than that for potassium, instead the Na^+ / v_{max} is lower than K^+/v_{max} ; the high affinity of KAAT1 for Na^+ possibly allows the midgut cells to uptake this ion even from the low concentrations (<5 mM) found in the lumen (200 mM).

Electrophysilogical data obtained in the past in our laboratory showed that the prestedy-state current, signalling rearrangements of charges in the membrane electricalfield, measured in the presence of K^+ 98mM is bigger that in a solution cointaining both K^+ and Na^+(5mM), condition that simulates the physiologicalenviroment. This behavior ensures the absorption of Na^+ which is lacking in the larvae diet.

As mentioned in the paragr. 1.4, KAAT1, similarly to several other transporters of the SLC6 family, displays uncoupled currents which are transmembrane currents observable in the absence of organic substrate. These currents show the following selectivity sequence: $Li^+ > Na^+ > K^+ \cong Rb^+ \cong Cs^+$ (Bossi *et al.*, 1999b;Peres & Bossi, 2000). Furthmore, in KAAT1 the selectivity order in high Na^+ conditions (98mM) is: Thr ≥ Pro > Met > Leu; in high K^+ the order is changed to Leu ≥ Met > Thr.

The potency order, in terms of amplitude of transport-assciated currents, depends on the driver cation; the substrate selectivity order changes depending on whether K^+ or Na^+ is the main bathing ion. Figure 1.13 indicates that whereas proline generates the largest currents in KAAT1 in the presence of Na^+ (*panel A*), this amino acid is the least effective in the presence of K^+. When the main ion present is K^+, (*panel B*) leucine is the amino acid producing the largest currents at all potentials.

The substrate competition experiments in KAAT1, performed by (Miszner *et al.*, 2007) indicate that leucine has a dominant role in the transport current that converges to that characteristic of leucine, even when other amino acids capable of larger currents. KAAT1 is able to complete the transport cycle in the presence of leucine, though with less efficiency if compared to other amino acids.

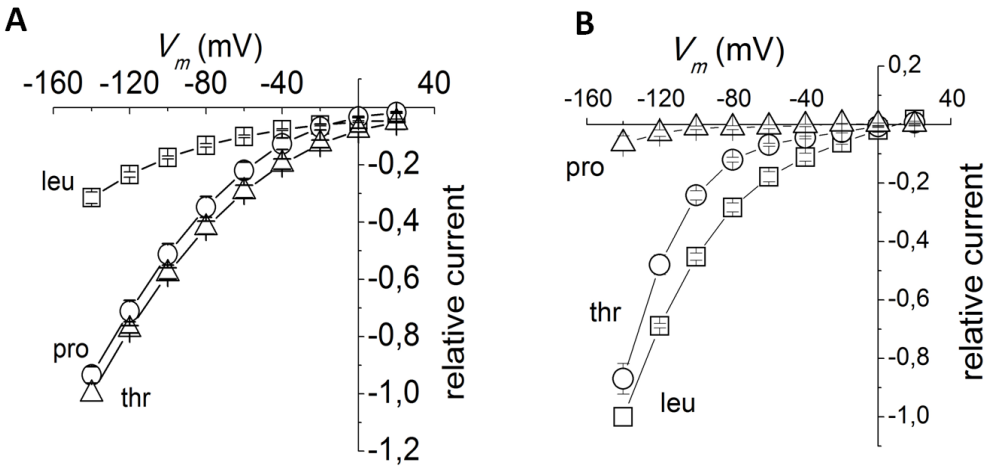

***Fig.1.13**: Transport- associated current (current in presence of substrate – current in absence) in presence of different substrates in KAAT1 in presence of Na^+ (A) or K^+ (B). All substrates were added at a concentration of 500 µM. Data are average currents ± SE from 3 to potassium (Soragna et al., 2004).*

Although studies addressing the anion dependence of amino acid transport in midgut brush border membrane vesicles did not reveal chloride dependence of (Hennigan *et al.*, 1993b), however, voltage clamp analysis showed that KAAT1 is Cl^- -dependent, because replacement of Cl^- by gluconate suppressed the amino acid evoked currents. This finding suggests a K^+ to Cl^- to amino acid stoichiometry of at least 2:1:1. The Cl- dependence of

KAAT1 indicates that there is not only a structural but also a functional similarity between KAAT1 and Na+ and Cl- dependent transporters of the GABA family.

In recent years, we have taken advantage of the special features of KAAT1 to investigate the structural/functional relationships within the NSS family. Sequence comparisons and site-directed mutagenesis studies have allowed us to identify structural determinants of transport activity such as residues involved in Na^+ and K^+ interaction and in amino acids translocation (Castagna *et al.*, 2009;Soragna *et al.*, 2004).

The research activity performed during my PhD course was mainly focused on the investigation of the functional role of an highly conserved sequence, extending from the extracellular loop 1 (EL1) to the transmembrane domain 2 (TM2) of KAAT1 in which three consecutive glycines (Gly85, Gly86, Gly87) are located. The degree of conservation in NSS transporters together with the structural localization suggests that this glycine triplet plays a relevant role in transport function; it is located at the extracellular side of protein, close one of the residues that participates in the external gate (Arg 30 in LeuT, Arg 76 in KAAT1, Fig.1.14A).

This region, highly conserved in SCL6 transporter family (Fig.1.14B), has already been studied individually in both GAT1 and SERT (Mao *et al.*, 2008;Zhou & Kanner, 2005) with a similar approach; in the two papers the role assigned to the glycine residues was different, suggesting that they might have a transport- specific task in each member of NSS family that could be related to the substrate transported.

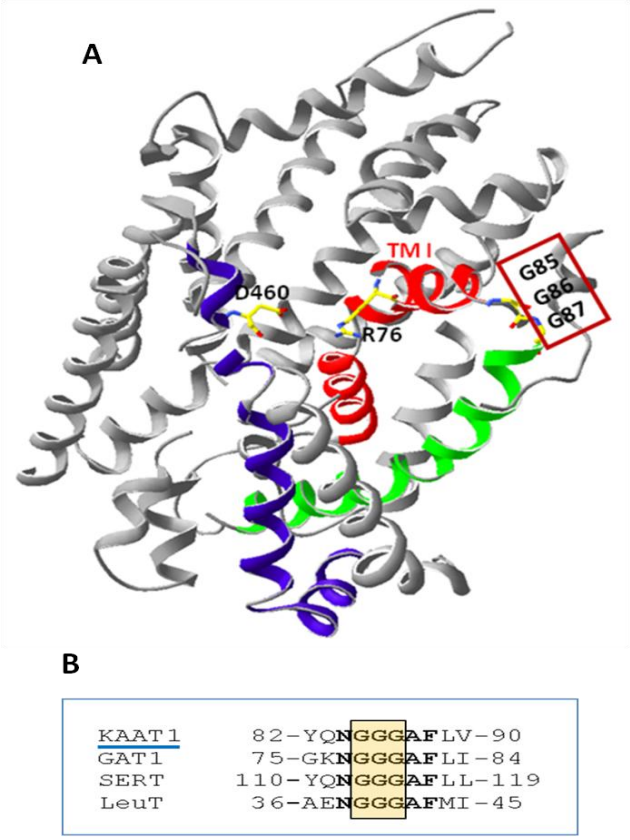

***Fig.1.14**: Homology modelling of KAAT1 structure based on the three-dimensional organization of LeuT. A: It is observable the spatial relationships of the glycine repeat with the residues forming part of the putative external gate of the transporter (Arg76 and Asp460 of 17 KAAT1). Gly85-87, Arg76 and Asp460 are depicted as ball and stick,TM1, TM2 and TM10 as ribbons, the rest of the structure as strands.*
B: Alignment of KAAT1, GAT1, SERT and LeuT sequences extending from Tyr82 to Val90 (KAAT1numbering) in which it is located the highly conserved glycine triplet.

The final part of my work was focused on the analysis of the relationships between temperature and substrate affinity. The purpose of this investigation was first of all to verify if KAAT1 substrate affinity was affected by temperature, similarly to the rat neuronal GABA transporter GAT1 previously investigated, and than to examine the overall efficiency of the transport, considering that while GAT1 is from mammalian (homeoterm) animals, KAAT1 originates from a poikilotherm inverterbrate (Castagna *et al.*, 2009).

Chapter 2

Materials and Methods

2.1 Molecular biology

2.1.1 Vectors for heterologous expression

Artificial plasmids are used for the gene cloning and expression and they represent an useful tool used to amplify and transfer foreign DNA inside an organism. Plasmids are double-stranded circular DNA that can replicate independently, the engineered plasmids for amplification show three common features:

- A replication origin, recognized by the host cell,
- A poli-linker or multi cloning site (MCS), composed by specific restriction sites grouped together, where it is possible to insert the DNA of interest
- A selective marker that make cells containing the plasmid able to be distinguished from the others. Generally are used genes conferring to the host a particular antibiotic resistance

The vector used to prepare the RNA for heterologous expression in *Xenopus laevis* oocytes needs to be constructed with the insert in specific position of sequences with different function. First of all, a promoter for the RNA-polimerase (T3,T7 or SP6); the transcription efficiency is also influenced by three more factors: a) the lack of initial codon (ATG), between promoter and the gene in order to avoid an early transcription; b) the lack of long non codifying DNA to limit the formation of secondary structures that may reduce the polymerase functionality; c) two post-transcriptional modifications: adding the cap at 5' and poliadenilation at 3'.

The Cap is a molecule of 7-metiloguanosine that protects the transcript from degradation and promotes the association of ribosomes with the 5' of mRNA. The poliadenilation consists in adding 150-300 adenosine at the 3'. The poly- A is not essential for transcription but it protects mRNA form ribonuclease and facilitates the transport of the mRNA from the nucleus to the cytoplasm.

2.1.2 KAAT1 cDNAs

KAAT1 was cloned from the midgut of the *Manduca sexta* larvae and it is 2881 bp long with an open reading frame of 1905 bp that coding for 634 amino acids (70 kDa) protein; the cDNA was insert between *NotI* and *SalI* in pSPORT1 (Fig.2.1), an expression vector that presents the β-lactamase gene conferring ampicillin resistance (AP^r) and the reported multi cloning site (MCS). At both ends of the MCS there are promotor sites for T7, T3 and M13 RNA polymerases.

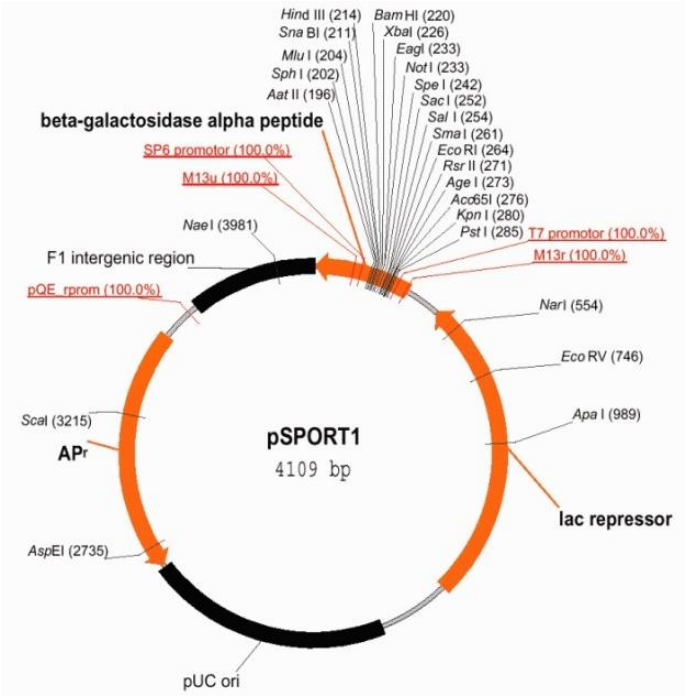

Fig.2.1: *pSPORT1 vector*

Another plasmid vectore used has been the pAMV-PA vector, shown in the Fig. 2.2, that it is a modified pBS (S/K^+) vector containing an alfalfa mosaic virus region directly upstream from the coding region of the insert At both ends of the MCS there are two promoter sites for either T7 or T3 RNA polymerases. The AMV sequence is used to promote the ribosomal attack. After the MCS there is a sequence coding for poly adenosine and a restriction site used to allow linearization (*NotI*) an useful procedure for the *in vitro* transcription of the cRNAs.

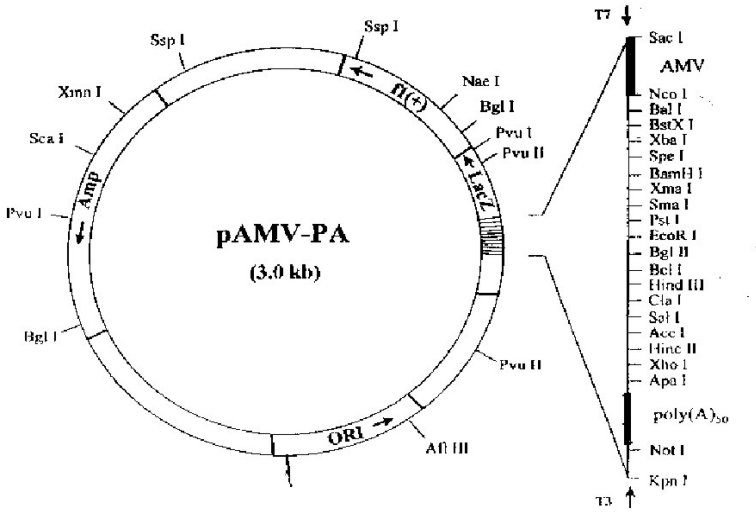

Fig.2.2: *pAMV-PA vector*

2.1.3 Flag-Epitope tagging

To allow optical measurements of the surface expression of the transporter proteins, a Flag epitope was inserted in a structural region considered not involved in the transport mechanism of KAAT1 cotransporter. In particular, the insertion was made into the second extracellular loop (EL2) close to transmembrane domains 3 (TM3) of KAAT1 (Fig.2.3), in correspondence of *PstI* site.

FLAG-tag is the first example of a fully functional epitope tag to be published in the scientific literature (Einhauer & Jungbauer, 2001) and it is a polypeptide protein epitope consisting of an eight amino acid peptide (Asp-Tyr-Lys-Asp-Asp-Asp-Asp-Lys). When it is inserted in a protein sequence, it can be recognized by a specific antibody, improving the identification.

The oligonucleotides encoding for the FLAG epitope were designed in order to contain the following nucleotide basis: i) the triplets encoding for the 8 amino acids of which FLAG is constituted (*highlighted in the sequence reported below*); ii) the basis representing the restriction sites for the *PstI* enzyme (*red colour*); iii) the nucleotides used to the annealing

of the flanking region, remaining in the sequence after enzymating cutting (*green colour*); iiii) two nucleotides to keep the FLAG sequence in frame (*pink colour*).

- Forward Primer:
  5'cta g**ct gca** **gat tat aaa gat gat gat gat aaa** **gct gca g**ga 3'
- Backward primer:
  3'gat c**ga cgt** **cta ata ttt cta cta cta cta ttt** **cga cgt c**ct 5'

After the digestion with the restrinction enzyme *PstI*, the construct KAAT-pAMV-PA was purified using the Wizard SV Gel and PCR Clean-Up System and incubated with SAP (Shrimp Alkaline Phosphatase 1U/µL, PROMEGA) at 37°C for 15 minutes, in order to completely dephosphorylate it.

The oligonucleotides encoding for the FLAG epitope were then ligated into the *PstI* site after annealing, in the KAAT1-pAMV-PA sequence; exactly, 1 µg of both the complementary oligonucleotides (forward and reverse) and sterile water were added to a reaction volume to 50 µL. The reaction mix was incubated for 2' minutes at 95°C and then cooled down to less than 25°C, in an suitable thermocycler. This step was used to optimize the next ligation reaction performed by T4-DNA ligase (Promega Italia, Milan, IT).

To ensure that the FLAG-tagged KAAT1-pAMV-PA construct was correctly inserted into the oocyte plasma membrane and it was functional, transport parameters were determinate by two electrode voltage clamp technique (explained in details in the next paragraphs), after the appropriate sequencing procedure.

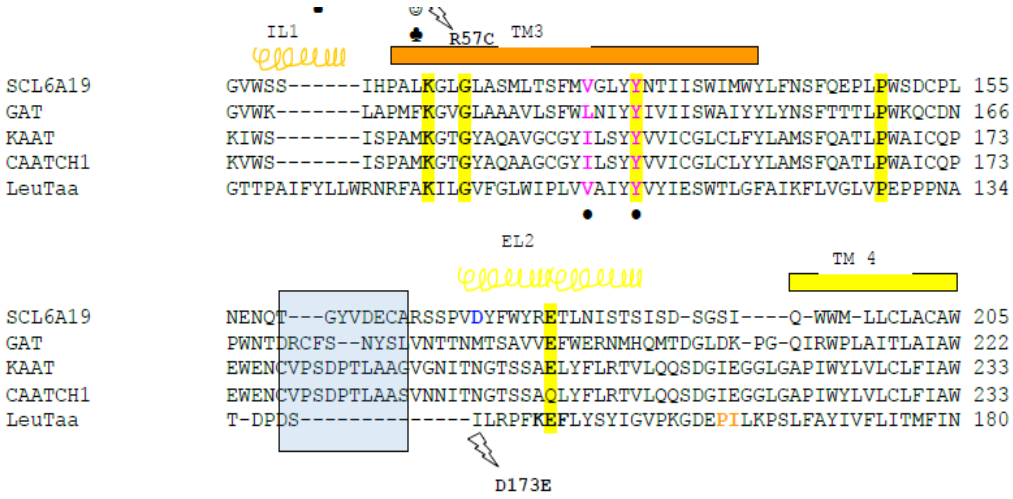

Fig.2.3: *KAAT1 amino acid region used for the FLAG insertion (see panel in grey colour).*

2.1.4 Alanine scanning mutagenesis

To test the functional importance of the stretch of glycines (Gly 85- Gly 87), highly conserved in the NSS transporter family, alanine scanning mutagenesis approach (Bennett *et al.*, 2000;Zhou & Kanner, 2005) was used; the technique was accomplished by the site-directed mutagenesis, obtained by PCR (Polymerase Chain Reaction) using hight fidelity DNA polymerase *Pfu* (QuikChange® Site-Directed Mutagenesis Kit, Stratagene Inc., Milan, Italy).

The following mutations were made: the individual substitution of each glycine with alanine; the conversion of the flanking residues Asn 84 and Ala 88 into glycine; the generation of the double mutants N84G/G87A and G85A/A88G, in order to obtain a shift of the triplet toward the N or the C terminus of the protein respectively.

Briefly, 20 ng of the plasmids containing respectively the KAAT1-pAMV-PA-FLAG and KAAT1-pSPORT1 cDNAs were amplified with 3 units of *Pfu* DNA polymerase, in the presence of the overlapping primers containing in their sequence the mutated codons:

G85A: 5'*-ct ttc atc gcg tac cag aat g**c**a gga ggt gc-*3'

G86A: 5'*-c atc gcg tac cag aat gga g**c**a ggt gct ttc-* 3'

G87A: 5'*-c cag aat gga gga g**C**t gct ttc ctg gtg cc-* 3'

A88G: 5'*-cag aat gga gga ggt g**g**t ttc ctg gtg cc-* 3'

G85A/A88G: 5’ *-**c**a gga ggt g**g**t ttc ctg gtg cct tac atc atc-* 3’

*N84G: 5’-ct ttc atc gcg tac cag **gg**t gga gga ggt gc-* 3’

N84G/G87A: 5’-ct *ttc atc gcg tac cag **gg**t gga gga g**c**t gc-* 3’

PCR amplification was performed with 25 thermal cycles of 95°C for 30 s, 55°C for 1 min, and 68°C for 14 min. Then, 10 units of *Dpn*I were added directly to the amplification reaction, and the sample was incubated for 1 h at 37 °C to digest the parental, methylated DNA. JM109 supercompetent cells were finally transformed with 1 µl of the reaction mixture and plated onto LB-ampicillin plates (for details, see below). After plasmid purification, plasmid cDNAs were fully verified by sequencing (Eurofin MWG Operon Biotech).

2.1.5 Plasmid amplification, extraction and purification

The vectors containing KAAT1 wt and mutant cDNAs were introduced into JM109 strain of *E. Coli* by the means of the heat-shock procedure following the instructions of the bacteria supplier (Promega). Transformed bacteria were then left to grow for about 1 h in SOC medium [tryptone 2% (w/v), yeast extract 0.5% (w/v), NaCl 10 mM, KCl 2.5 mM, glucose 20 mM], centrifuged, plated on dishes (Petri) containing selective medium (LB-Agar added with 50 µg/ml ampicillin) and incubated over night at 37°C. The day after, colonies were picked up and inoculated in liquid selective medium (LB added with 50 µg/ml ampicillin). Bacteria were left to grow over night at 37°C and then the plasmid DNA was extracted using Wizard® *Plus* SV Miniprep (Promega) following supplier’s instruction. The extracted DNA was loaded on a 1% agarose gel in TAE 1X buffer to check the quality and to estimate the concentration.

2.1.6 mRNA preparation

In order to achieve an efficient *in vitro* transcription, the clone containing the cDNA of interest has to be linearized in 3’ direction with respect to the coding region. The cDNA encoding for the transporter isoforms of interest was linearized with *Not*I enzyme. Briefly, 8-10 µg of plasmid DNA were digested, then purified using the Wizard® SV Gel and PCR

Clean-Up System (Promega) and eluted in 35 µl of nuclease free water. 3 µl were loaded on a 1% agarose gel in TAE 1X buffer to check the linearization. The remaining DNA was used for the *in vitro* transcription as described previously in detail {Bossi, 2007 7200 /id}. Briefly, the linearized DNA was incubated at 37°C for 3h in presence of 200 units of T7 RNA polymerase, 18 µl of 5X Trascription Buffer, 8 µl of 100 mM DTT, 2.5 µl of RNasin 30 U/µl, 13 µL NTPs mix (ATP, CTP, UTP 10 mM and GTP 0.5 mM), 6.5 µL of 10 mM Cap Analog (Promega), 10 µl RNA polymerase 20 U/µl (final volume 90 µL). After 10, 20, and 40 min from the beginning of the incubation, 1 µL of 25 mM GTP was added to the reaction. After 1 h from the start of the transcription, a mixture of 4 µl of 5X TB, 1 µl of 100 mM DTT, 1 µl of RNasin 30 U/µl, 5 µl of NTPs mix, 1 µl of T7 RNA polymerase 20 U/µl, 1 µl of 25 mM GTP, 4 µl of nuclease-free water was added to each sample. After three hours, the reaction was stopped by adding nuclease-free water to a volume of 200 µl. All enzymes were supplied by Promega Italia, Milan, Italy.

The transcribed cRNA was extracted with phenol:chloroform:isoamyl alcohol, 25:24:1, pH 6.6, precipitated with LiCl 8 M and washed with 70% EtOH. The dried cRNA was then resuspended in a small volume of nuclease-free water and the concentration estimated using a spectrophotometer (1 A_{260nm} unit = 40 µg/ml).

Transcribed cRNAs had a modifications which mimic *in vivo* conditions: the process of 5' capping. The so called "Cap Analog" is a modified guanine (m^7G(5')ppp(5')G) which, although is not necessary for the protein expression, increases the translation efficiency and also protects the mRNA from degradation.

2.1.7 Heterologous expression in oocytes

2.1.7.1 Frog maintenance

Expression systems yield a really high number of copies of the protein that allow precise biochemical and electrophysiological measurements. In this work, *Xenopus laevis* oocytes have been used as a very convenient heterologous expression system for the cotransporter KAAT1 and the mutants.

Xenopus laevis is a member of the Pipidae family originally from South Africa and able to adapt to the laboratory conditions. *Xenopus* females are kept in the animal house in dark plastic aquaria containing chloride-free water, because chloride causes the inactivation of

magainine, an antibiotic that helps the epidermis prevent bacterial infections. The water needs to be changed every three days and the animals showing infections must be isolated and treated. The water temperature is kept between 18 and 21°C. The salinity must be controlled to avoid the loss of salts from epidermis and it is necessary to provide a light-dark cycle of 12 hours, in order to attenuate the natural annual cycles thus limiting variability in oocytes production.

The frogs nutrition was carried out according to the institutional and national ethical guidelines.

2.1.7.2 Oocytes usefulness, isolation and selection

Xenopus laevis oocytes are a powerful expression system (Fig.2.4) with numerous advantages: i) high expression rate of exogenous proteins (even after only 18 hours); ii) an efficient biosynthetic apparatus which allows all post-translational modifications necessary for the functionality and the correct targeting of the protein; iii) high density of proteins produced upon cytoplasmic mRNA injection; iv) dimensions appropriate for easy microinjection and voltage clamp; v) easiness to maintain in culture for relatively long periods (up to ten) with no particular sterile conditions; vi) possibility of coexpression of different proteins in various combinations by simply co-injecting the respective cRNAs; vii) low expression levels of endogenous membrane proteins (the endogenous channels have been well characterized, thus it is easy to distinguish them from the injected proteins).

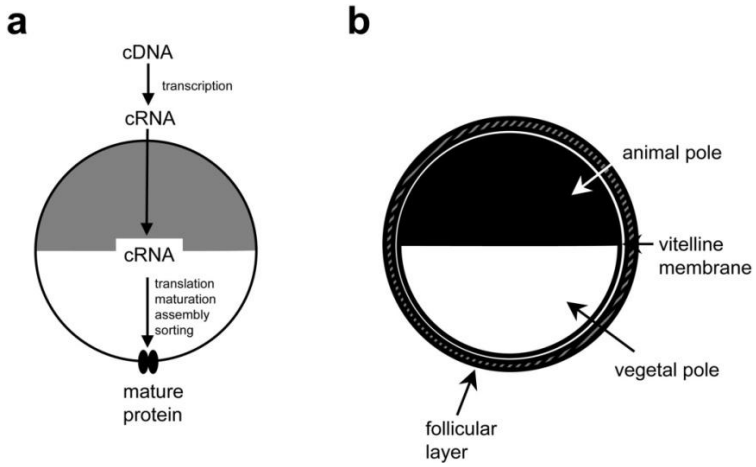

Fig.2.4: *Exogenous protein expression in Xenopus laevis oocytes.*

Xenopus oocytes have also some disadvantages: i) the expression of exogenous protein is transient; ii) the ideal temperature for their survival (about 18°C) is usually lower than the temperature appropriate for exogenous proteins (37°C for mammalian proteins) and this can affect the folding process; iii) although quiescent cells, oocytes possess their own genetic ensemble which might interfere with the exogenous proteins.

Oocytes were prepared as previously described (Bossi *et.al*., 2007).They were obtained from adult female *Xenopus laevis*, the frogs were anaesthetised in MS222 (tricaine methansulfonate) 0.10%(w/v) solution in tap water and portions of the ovary were removed through an incision on the abdomen. The oocytes were defolliculated by treatment with collagenase (Sigma Type IA), 1 mg/ml in ND96 Ca^{+} free, for at least 45' at 18°C . After 24 hours at 18°C in modified Barth's saline solution (MBS), the healthy looking selected oocytes were injected with 50 nl of the transporter cRNA diluted to a final concentration of 0.25 µg/µl for a quantity of 12,5 ng per oocyte, using a manual microinjection system (Drummond). The oocytes were then incubated at 18°C for 3-4 days in MBS before electrophysiological studies; during incubation the solution was changed every 24 hours.

The experiments were carried out according to the institutional and national ethical guidelines.

2.2 Protein localization

2.2.1 Single-oocyte chemiluminescence

Surface expression of the tagged transporter isoforms was determined by the single oocyte chemiluminescence (SOC) technique (Zerangue *et al.,* 1999;Rauh *et al.,* 2010;McAlear *et al.,* 2006), that employs enzyme amplification with a chemiluminescent substrate and sensitive linear detection with a luminometer. A monoclonal primary antibody anti-Flag M2 (Sigma F3165,10 µg/ml) and goat anti-mouse IgG secondary antibody labeled with HRP Jackson ImmunoResearch Laboratories) were used to detect the plasma membrane expression.

The oocytes expressing different FLAG-KAAT1 isoforms, as well as non-transfected oocytes, were washed twice for 5 min in ice-cold ND96 pH 7.6 and fixed with 4% paraformaldehyde in ND96 for 15 min, rinsed 3×5 min with equal volumes of ND96, and then incubated for 1 hour in a 1% BSA-ND96 blocking solution (used in subsequent antibody incubation steps), 1 h in mouse anti-FLAG M2 1 μg/ml in 1% BSA-ND96, washed 6x3min in 1% BSA ND96, incubated for 1 hour in peroxidase-conjugated goat anti-mouse IgG 1 μg/ml, IgGHRP (Jackson ImmunoResearch Laboratories), washed 6x3min in 1% BSA-ND96 and then 6x3min in ND96 alone. For chemiluminescence readings, oocytes were transferred into a 96 wells plate (Assay Plate White not treated flat bottom-Corning Costar) filled with 50 μl SuperSignal Femto (Pierce). Luminescence was quantified with a Tecan Infinity 200 microplate reader. The plates were read not later than 5 minutes after the transfer of the first oocyte. The data were then acquired at least three times in 10 minutes and for each oocyte the mean of three readings was calculated. Results were normalized to the mean value of wild-type FLAG-KAAT1 for each batch and are given in relative light units (RLU).

2.3 Electrophysiology and data analysis

Membrane electrophysiology has several advantages over other techniques used in transport studies: i) the membrane voltage of the cell is under control; ii) the temporal resolution is high; iii) the results may be obtained immediately, data can be analyzed and interpreted in real-time, and consequently the protocols can be changed or adjusted during the same experimental session. These benefits may be exploited in the study of transporters, thereby adding valuable information and significantly increasing efficiency. The activity of electrogenic transporters, that translocate electrical charge, by definition, during their working cycle, is strongly influenced by the transmembrane potential. Thus, tracer flux experiments suffer from some uncertainty, because the membrane voltage is not under control, and not only the value of the electrical gradient is unknown, but it is also bound to change as a consequence of the electrogenic activity of the transporter itself. A more reliable evaluation of the activity of the transporter is obtained instead when the membrane potential is “clamped”.

2.3.1 Two-Electrode Voltage-Clamp (TEVC)

Transport currents generated by the activity of KAAT1 wt and mutants were investigated by classical two-electrode voltage clamp experiments.

The "voltage-clamp" technique was introduced by Marmont and Cole (Cole *et al*., 1941) and by Hodgkin, Huxley and Katz (HODGKIN *et.al*., 1952) to study the ionic currents underlying the action potential in nerve axons, and it has been extended to the study of transporters soon after the cloning and expression of the first transporters in *Xenopus laevis* oocytes (Hediger *et al*.,1987;Ikeda *et al*., 1989;Parent *et.al*, 1992;Mager *et.al*, 1993). The TEVC technique is based on the use of two microelectrodes, one for recording the transmembrane voltage and one for passing current (Fig.2.5). The recorded membrane voltage is compared to the desired (command) voltage and a compensating current is automatically injected into the cell by the appropriate electronic apparatus. In this technique the independent (controlled) variable is the membrane voltage, controlled by the experimenter, while the dependent (measured) variable is the membrane current.

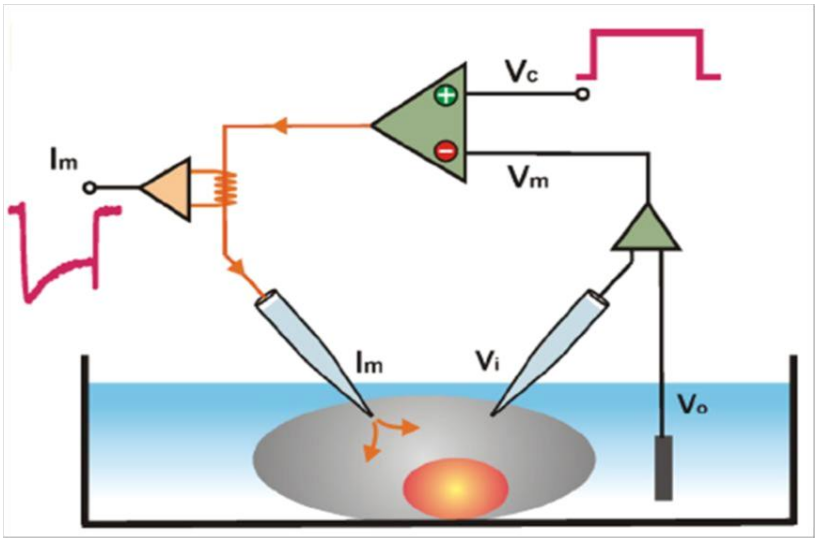

***Fig.2.5**: Two electrode voltage clamp. I_m is the membrane current, V_i is the membrane voltage and V_c is the command voltage.*

When a current takes place due to the activity of the transport systems located in the membrane, a negative feedback in the circuitry injects into the oocyte a current that exactly compensates the charge flow trough the cell membrane, in order to maintain transmembrane voltage under control. In addition to keeping the membrane potential constant, membrane voltage changes of any desired form can be applied to the cell by the TEVC technique. In the case of ion-coupled transporters, the transmembrane current is an indication of the transport activity, and the possibility of accurately controlling the membrane potential is particularly crucial in voltage-dependent processes.

2.3.2 TEVC experimental setup

A schematic view of the TEVC experimental setup used in this work is shown in Fig.2.6.

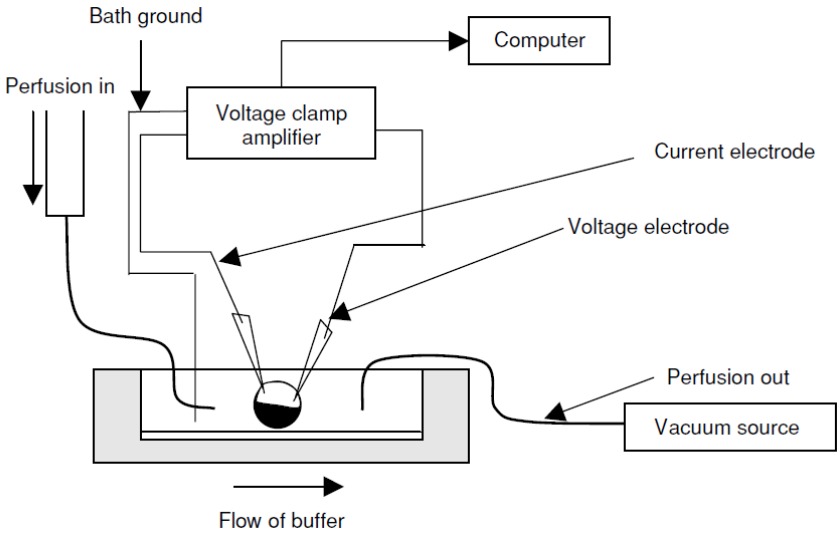

Fig.2.6: *Schematic representation of the experimental setup*

The voltage-clamp amplifier (GeneClamp, Axon Instruments Foster City, CA, USA or Oocyte Clamp OC-725B, Warner Instruments, Hamden, CT, USA) was connected to a computer through an AD/DA (analog-digital, digital-analog) converter (DIgiData 1200, Axon Instr.). This device converts the analog signal from the amplifier to a digital signal intelligible for the computer, and vice versa. Usually, signals derived from the amplifier were also displayed on an oscilloscope (TDS 420, TekTronix Inc., Beaverton, OR, USA).

A dissection microscope (Wild M3B, Leica Microsystems AG, Wetzlar, Germany) was used to visualize the oocyte and micromanipulators (MM-33, Märtzhäuser Wetzlar GmbH & Co. KG, Wetzlar-Steindorf, Germany) were use to move the electrodes. A perfusion system consisting of a set (16) of syringes was used to deliver the various solutions to the unique solution inlet of the chamber (a modified version of RC-1Z, Warner Instr.). All the syringes were connected to the inlet by the use of two manifolds (MP-8, Warner Instr.) and were all positioned at the same height in order to have the same flow rate for each solution. The recording chamber has a small volume (about 200 μl, 85 *m*l/mm height) which allows a rapid solution exchange (about 8-10 seconds in our system). The solution is aspirated by a modified acquarium pump through a suction reservoir connected to the oocyte well. The oocyte was impaled by two intracellular glass microelectrodes filled with KCl 3 M and having tip resistances between 0.5 – 4 MΩ. These resistance values were usually obtained by gently breaking the tips on the bottom of the chamber. Agar bridges (3% agar in 3 M KCl) connected the bath electrodes to the experimental chamber.

All the equipment needed for the recording (dissection microscope, perfusion system, oocyte chamber, micromanipulators and reference electrode) is placed inside a Faraday cage, in order to reduce the noise derived from electromagnetic fields, and on an anti vibration table. The cage and all the instruments inside of it were grounded.

2.3.3 Protocols and data analysis

In voltage-clamp mode the holding potential (V_h) was generally -60 mV (-80 mV for Na^+ dependence experiments).

The voltage pulse protocol used, consisting in hyperpolarizing and depolarizing jumps, consisted of 200 ms pulses to test potentials from -160 to +40 mV in 20 mV increments (four pulses were averaged at each potential), or in a staircase protocol consisting of nine 20 mV steps to test potentials from -140 to +20 mV. The current signal was filtered at 1 kHz before sampling at 2 kHz.

The currents remaining after subtraction of the traces recorded in absence of substrate from those in its presence were assumed to represent the transport-associated currents. In order to compare data derived from different oocytes (with different expression level) or from

oocytes from different batches, transport-associated currents were usually normalized at the maximum current value recorded at the more hyperpolarized membrane potential used. When the substrate was missing transient currents could be recorded. The isolated traces were fitted with single exponentials to obtain the time constant of decline, and integrated to calculate the amount of displaced charge, after zeroing any residual steady-state transport current.

The experiments were run under the WinWCP version 4.4.6 software (J. Dempster, University of Strathclyde, UK, 2012). Data were analyzed using Clampfit 10 (Molecular Devices, LLC, Sunnyvale, CA, USA, 2012) while figures were prepared with Origin 8 (OriginLab Corp., Northampton, MA, USA, 2008).

2.3.4 Extracellular Solutions

The oocyte culture and washing solutions had the following composition (in mM), ND96: NaCl 96, KCl 2, $MgCl_2$ 1, $CaCl_2$ 1.8, Hepes 5, pH 7.6; MBS: NaCl 88, KCl 1, $NaHCO_3$ 2.4, Hepes 15, $Ca(NO_3)_2$ 0.30, $CaCl_2$ 0.41, $MgSO_4$ 0.82, sodium penicillin 10 µg/ml, streptomycin sulphate 10 µg/ml, gentamycin sulphate 100 µg/ml, nystatin 10 U/ml, pH 7.6; PBS: NaCl 138, KCl 2.7, Na_2HPO_4 8.1, KH_2PO_4 1.9, pH 7.6. The external control solution during the electrophysiological recordings) had the following composition (mM): NaCl, 98; $MgCl_2$, 1; $CaCl_2$, 1.8, Mes 5mM. In the others solutions NaCl was replaced by LiCl, KCl or TMACl. The final pH value (7.6) was adjusted with HCl and NaOH. For the sodium dose-response experiment, Na^+ was substituted by equal amounts of tetramethylammonium (TMA); the Na^+ concentrations used were 0.3, 1, 3, 10, 30, 60 and 98 mM. Amino acids (leucine, threonine, proline) at the saturating concentrations (3 mM for proline and threonine, 1 mM for leucine) were added to the same solutions to induce transport-associated currents. In the substrate dose-response experiments, the concentrations were 3, 10, 30, 100, 300 and 1000 µM for threonine and 3, 10, 30, 100, 300 and 1000 µM for GABA. All the substrate were dissolved in sterile water and then added to the appropriate solution.

The oocyte was perfused continuously in a rapid solution exchange chamber (Warner Instruments model RC-1Z, http://www.warneronline.com/), with a washout time of about 1 s.

Experiments were performed at room temperature (20–25 °C) except during the studies on the effects of temperature in which a range of temperature (20-30^{o}C) was used. In this case, cold solutions in the reservoirs were heated to the desired temperature just before entering the recording chamber. A TC-344A in-line heater controller (Warner Instr. Corp., Hamden, CT, USA) with feedback control of the temperature was used. The actual temperature in close proximity of the oocyte was continuously monitored through a second thermistor placed in the bath.

2.4 Radiolabeled amino acid uptake

Besides the recordings of electric signals generated during functioning, another useful approach to derive information about the transport process is certainly the *uptake* of radiolabelled substrates (amino acids).

All the uptake data presented in this thesis were obtained in collaboration with the group of Prof. V.F.Sacchi, Dipartimento di Scienze Farmacologiche e Biomolecolari, Università degli Studi di Milano, Milano, Italy).

Amino acid uptake was evaluated 4 days after injection. Groups of 8-10 oocytes were incubated for 60 min in 120 µl of uptake solution 100 mM NaCl, 2 mM KCl, 1 mM $CaCl_2$,1 mM $MgCl_2$, 5 mM Hepes/NaOH, pH 8) with 0.1 mM [^{3}H]leucine (444 kBq/ml, specific activity 3.996 Tbq/mmol) or 0.1 mM [^{3}H]proline (592 kBq/ml, specific activity 2.775 TBq/mmol) (all from PerkinElmer Life Sciences). Alternatively, to evaluate the uptake induced in the presence of lithium or potassium ions, NaCl was substituted by 100 mM LiCl or 150 mM KCl respectively. All uptake experiments were made at room temperature. After incubation oocytes were rinsed with ice cold wash solution (100 Mm choline chloride, 2 mM KCl, 1 mM CaCl, 1 mM $MgCl_2$, 5 mM Hepes/ choline hydroxide, pH 8), and dissolved in 250 µl of 10% SDS for liquid scintillation counting.

KAAT1 induced uptake was calculated as the difference between the mean uptake measured in cRNA- injected oocytes and the mean uptake measured in non-injected oocytes.

Chapter 3

Results

As mentioned in the *Introduction* section, KAAT1 is the first invertebrate amino acid transporter cloned in 1998, that using K^+, in addition to Na^+ as driving ion, transports a wide range of neutral amino acids. It is 30% identical to the GABA transporter GAT1 which is the prototype of the Na^+/Cl^- dependent transporters family to which it clearly belongs (Castagna *et al.*, 1998). For this reason, it may represent a very useful study-model for the understanding of structure-function relationships.

Due to its electrogenic amino acid uptake (Liu *et al.*, 2003) and an amino acid selectivity (Feldman *et al.*, 2000;Soragna *et al.*, 2004) activated and influenced by the driving ions, one of the best ways to study the functionality appears to be electrophysiology, by the TEVC (Two Electrode Voltage Clamp) on *Xenopus laevis* oocytes injected with cRNA coding for the transport protein. This technique, with respect to other measurements, has the principal advantage that the currents generated by heterologously expressed transporter proteins are measured keeping the electrochemical gradient under control. Moreover, different conditions may be tested on the same cell, producing better comparison of effects. Thirdly, some of the results may be available immediately allowing more efficient planning of the experiments; finally, the analysis of the electrophysiological data makes it possible to obtain different parameters related to the transport activity of the protein. For example, the apparent affinity for the substrate, its turnover rate, etc.

Classical studies on whole cells (Christensen, 1990) had shown that the electrical charge of an amino acid plays a critical role in its interaction with the transporters; information from sequence analysis and site-directed mutagenesis may lead to the identification of specific amino acid residues that are important for the transport function of KAAT1 (Sacchi *et al.*, 2003).

In this work, the attention was focused on the study of the functional role of a highly conserved sequence, extending from the extracellular loop 1 (EL1) to the transmembrane domain 2 (TM2) of KAAT1 in which three consecutive glycines (Gly85, Gly86, Gly87) were found.

The aim was to evaluate the idea that one or more of the native glycine residues, highly conserved in the NSS/NAT family, might play a role in conformational transitions during the transport. Most of the functional information, i.e transport activity, apparent affinity for sodium, interaction with different cations, were derived from electrophysiological measurements and also from uptake experiments in the absence of control of the

membrane voltage. Furthermore, to better understand the structure-function relationships, additional details were obtained about the correct targeting to the plasma membrane of the glycine mutants, performing optical measurement of the surface expression by the single oocyte chemiluminescence (SOC) technique pioneered by Zerangue (Zerangue *et al.*, 1999) and used by others (Haerteis *et al.*, 2009;Bossi *et al.*, 2011).

The second part of my PhD work was focused on the analysis of the relationships between temperature and substrate affinity in the ion-coupled cotransporter KAAT1 in comparison with GAT1, and in particular I have investigated the rate of transport and the effects on the presteady-state currents, i.e. the electrical signal arising from the initial steps of the transport cycle (Parent *et al.*, 1992;Mager *et al.*, 1998;Bossi *et al.*, 1999a).

3.1 KAAT1: the functional role of the highly conserved glycines triplet

Within the NSS family, certain regions of the sequence have particularly high incidence of identity at the amino acid level; the strongest regions of identity appear to be in the TM1, TM2 and EL1, the region between the two TMs that have been examined in SERT(Mao *et al.*, 2008) and in GAT-1(Zhou & Kanner, 2005), in the context of a specific glycine mutation. From mutagenesis experiments carried out in the conserved glycine triplet region in GAT1 and SERT by Zhou Y. and Kanner in 2005 and Mao Y. and co-workers in 2000, respectively, it has been inferred that there is a relevant role of the glycine residues in the transport activity. In this context, the peculiarity of KAAT1 to be able to transport a wide spectrum of neutral amino acids with a potency order related to driver cation (Soragna *et al.*, 2004;Miszner *et al.*, 2007), makes it appropriate to further investigate the role of this highly conserved sequence. Interesting observations arise when the glycine triplet of KAAT1 is compared to those of the mammalian members of the Na^+/Cl^- family of cotransporters, listed above.

Glycine can introduce flexibility in the protein structure, and in 2002 Jiang Y. and co-workers (Jiang *et al.*, 2002)showed a glycine residue may act as a gating-hinge in potassium channels; furthermore, other evidences have been presented suggesting that

glycine residues engineered into the proton-coupled lactose transporter confer conformational flexibility to it (Leyland & Dart, 2004).

3.1.1 Cell surface expression of glycine mutants

To test the functional importance of the stretch of glycines (Gly 85- Gly 87) highly conserved in the NSS transporter family, the alanine scanning approach has been used to get the following mutations: the substitution of each residue with alanine; the conversion of the flanking residues Asn 84 and Ala 88 into glycine; the generation of the double mutants N84G/G87A and G85A/A88G in order to obtain a shift of the triplet toward the N or the C terminus of the protein respectively.
In order to analyze their surface expression, we have inserted in the sequence of the KAAT1 transporter, a FLAG epitope (Asp-Tyr-Lys-Asp-Asp-Asp-Asp-Lys), (see *Method* section, *Chapter 2*) which did not alter its functionality. For the Flag insertion in the sequence of KAAT1, we have considered as the best "candidate" an extracellular region, of KAAT1, with the smallest functional role, high hydrophobicity and the least homology with the other carriers of the family.

Insertion of the FLAG epitope did not alterate KAAT1 transport activity

Starting from an holding potential of -60mV and following the protocol which provided a jump of 20 mV every 200 ms, first in the hyperpolarizing direction (until -140 mV) and then in the opposite direction, up to 40 mV, the electrophysiological behavior observed in FLAG-tagged KAAT1 wild type was almost identical to the not tagged one, both in Na^+ and in K^+, in the presence of the substrates threonine and proline at the saturating concentrations (3mM and 1mM, respectively); this demonstrated its correct insertion into the membrane (Fig.3.1).

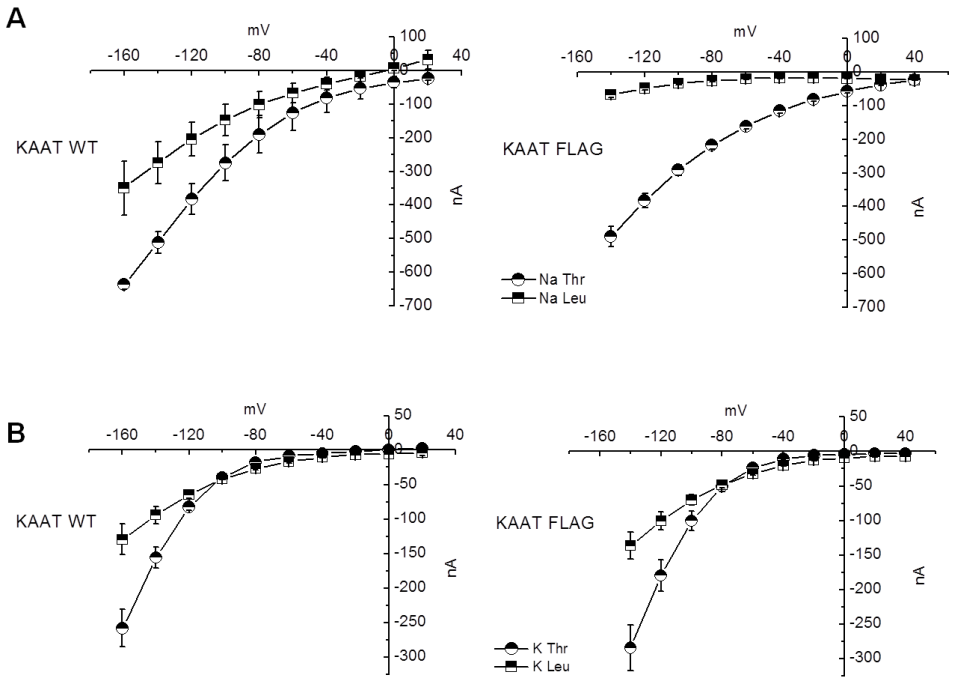

***Fig. 3.1**: I/V relationships of KAAT1 WT and KAAT FLAG, in presence of Na^+ (A) and K^+ (B), and with the addition of the indicated substrates to the high concentration solutions.*

To obtain the transport-associated currents, the traces recorded in the absence of the substrate were subtracted from those recorded in the presence of the same. From the *I/V* graphs, it was evident that there was just an insignificant difference in the behavior of the KAAT FLAG with respect to wt.

In the right panel (Fig.3.1), in Na^+, it is evident as the currents elicited by leucine appeared smaller than those elicited by threonine, especially for hyperpolarizing potential.

Analysis of the Mutants surface expression

After testing the functionality of the KAAT1 FLAG, the quantitative expression of the glycine mutants transporters in the oocyte membrane was verified. The mutants generated by alanine scanning mutagenesis (see in *Chapter 2*) were expressed and functionally characterized using the *X. laevis* oocytes; the single-oocyte chemiluminescence (SOC) technique (portrayed in *Method* section) was used to quantify the luminescence signal proportional to the expression on the plasma membrane.

As shown in Fig. 3.2, the single mutants showed a surface localization comparable to wt with the only exception of G85A and G87A that were present at the plasma membrane at a 50% level. The same level of expression for the double mutant G85A/A88G was observed, while N84G/G87A mutant was completely undetectable in the oocyte membrane. The chemiluminescence was detected from 20 to 40 oocytes from 5 different batches expressing the wt and the indicated mutants of KAAT1-FLAG and secondarily labeled with peroxidase-conjugated goat anti-mouse (IgG-HRP) are shown. The data were normalized to the mean value of the wild-type FLAG-KAAT1 of each batch.

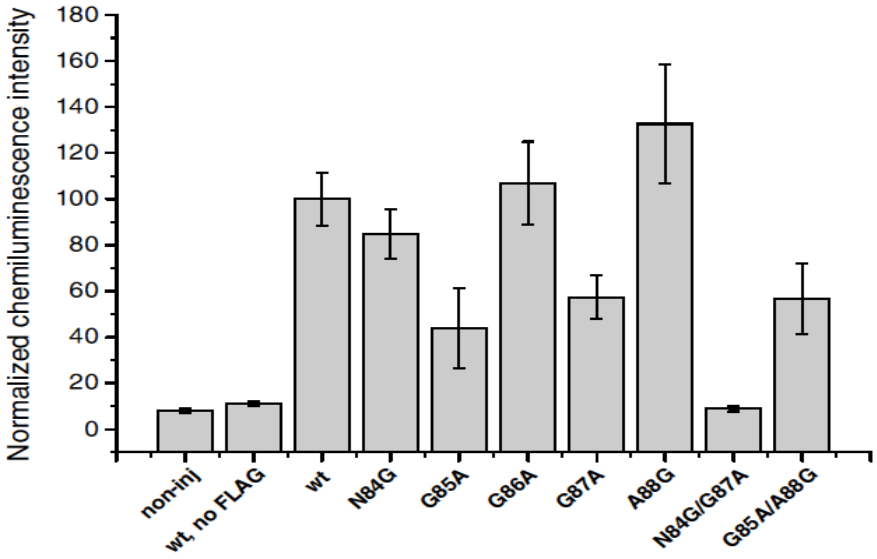

***Fig.3.2**: Membrane expression of KAAT1wt and mutants.*

3.1.2 Analysis of the Transport activity

Radiolabeled amino acid uptake

Figs 3.3 *A and B*, show the data obtained from the amino acid uptake evaluated in glycine mutants, 4 days after mRNA injection, to compare the ability to transport its substrate to that of the wild-type. It can be observed that in the presence of a Na^+ gradient, G85A, G86A, G87A mutants showed 0.1 mM leucine uptake reduced of the 40-50% compared to the wild type; the same percentage of uptake reduction it was showed from the mutants in

0.1 mM proline, with the exception of G87A that induced a comparable uptake, despite the 50% surface expression reduction (Fig. 3.2). The amino acid uptake reduction of G85A mutant was concordant with its reduced surface expression.

As shown in Fig. 3.4A, in the presence of 3mM proline, N84G mutant showed a residual transport activity (30% of wt), whereas that of A88G, G85A/A88G and N84G/G87A mutants was less than 10% of wt; the data relative to the last one would be in agreement with its almost undetectable expression on the plasma membrane.

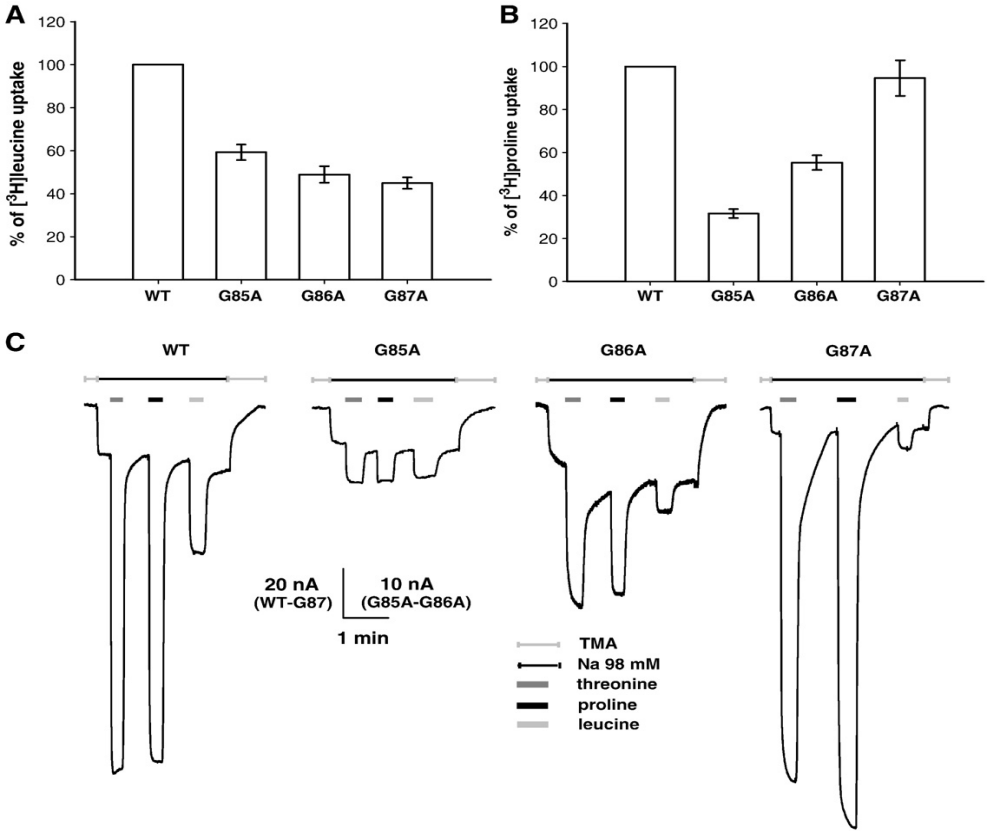

***Fig.3.3**: Amino acid uptake and transport associated currents in oocyte expressing the indicated glycine mutants in the presence of a Na^+ gradient: Bars represent 0.1 mM leucine (A) or 0.1 mM proline (B) uptake expressed as percentage of wt and are means ± S.E. of at least 30 oocytes from 3 different batches. C: representative oocytes expressing wild type. KAAT1 and each of glycine mutants. tested at the voltage to -60 mV in TMA solution (light gray lines), then changed in Na solution (black lines). The substrates, threonine 3 mM (dark gray bars), proline 3 mM (black bars) or leucine 1 mM (light gray bars) were added after stabilization of current in sodium. Before applying the second and the third substrates, the complete recovery to the starting value of the current in sodium was waited.*

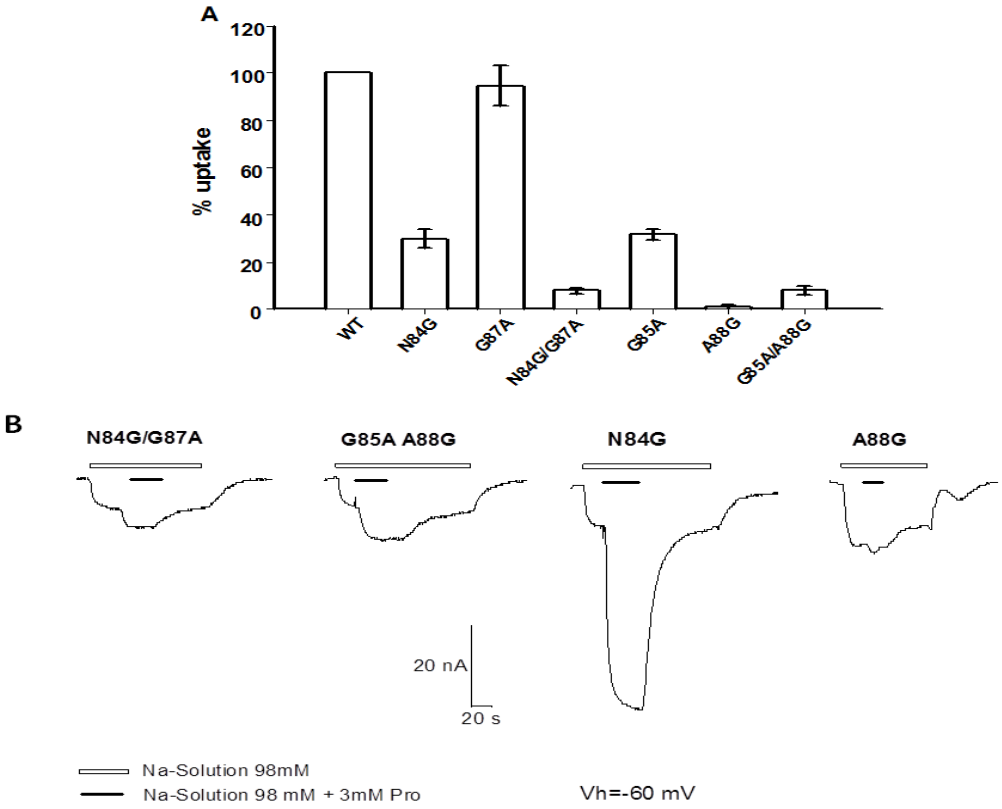

Fig.3.4*: Amino acid uptake and transport associated currents in oocyte expressing the indicated glycine mutants in the presence of a Na^+ gradient: Bars represent 0.1 mM proline (A) uptake expressed as percentage of wt and are means ± S.E. of at least 30 oocytes from 3 different batches. B: representative oocytes expressing wild type KAAT1 and each of others glycine mutants tested at the voltage to -60 mV in Na solution (white lines). The substrate proline 3 mM (black bars) was added after stabilization of current in sodium.*

Transport-associated currents

The transport cycles of many members of secondary-active ions cotransporters are electrogenic, whereby net charge transfer accompanies cotransport and the partial reactions that constitute the transport cycle show voltage dependent kinetics (Andrini *et al.*, 2008). Electrophysiological data illustrated below include different current types that are

measurable when an electrogenic transport protein is analyzed. When the proline was transported by the G87A mutant (Fig.3.3 C) an uncoupled current (Peres & Bossi, 2000) was measured; it was observable in the presence of both driven and driving substrates and it usually manifests itself as a current in excess of that associated with the stoichiometric charge translocation (Andrini *et al.*, 2008;Perez-Siles *et al.*, 2011). The cotransporters, in general, can show one or both type of uncoupled currents (Perez-Siles *et al.*, 2011) but there are also reported a transport associated current and a leak current; the definition of which is explained in *Chapter 2.*

All the oocytes in the experiments here reported were tested 72h after the cRNA injection in the presence of NaCl 98 mM and TMA (tetramethylammonium). Figure 3.3C shows records of membrane currents from representative oocytes expressing KAAT1 wild type and each of single glycine mutants, tested under controlled and fixed voltage of -60 mV, and exposed to three different substrates (threonine and proline, at the same saturating concentration of 3mM, and leucine 1mM).

As expected, the different amino acids are able to generate transmembrane currents; it is known (Bossi *et al.*, 2000;Bossi *et al.*, 1999b) that the KAAT1 wt's selectivity order in high Na^+ conditions (98mM) is: Thr ≥ Pro > Leu, while in high K^+ the order is changed to Leu > Thr.

For all the three mutants, leucine application induced an inward transport current that was 20-40% of that of the wt protein; the same happened for the G85A and G86A mutants, when threonine or proline were perfused, while the application of these last two substrates elicited in the G87A mutant an inward current similar to that of wt or larger (mainly in presence of proline).

Fig.3.4 shows records of membrane currents from representative oocytes expressing KAAT1 wild type and each of others glycine mutants tested under the same voltage conditions mentioned above and exposed to the substrate proline 3 mM, whose application induced a small inward transport current, approximately of the 10-20% of that the wt protein (*not shown*) in all the three mutants, with the only exception of the N84G mutant. In presence on the substrate here added, it generated an inward current comparable to that of wt.

Figure 3.5 illustrates the results obtained from more detailed investigation of the electrophysiological behavior over a larger voltage range. The current-voltage (*I/V*)

relationships show that the transport-associated current induced by leucine was highly impaired in all mutants; whereas it can be observed a G87A's behavior similar to the wt, when the substrate was threonine. Replacing the last with the proline , the current generated by the G87A mutant was increased, as it happened at the fixed voltage experiments. These data, calculated as the difference of the traces recorded in the absence from those in the presence of the substrate indicated below, consolidate the previous ones. A correlation with the uptake data shown above (Fig.3.4B) is supported also from the result illustrated in the panel left bottom (Fig.3.5), where it is possible to observe that the transport current induced by proline was greatly impaired in all mutants, except in the N8AG isoform.

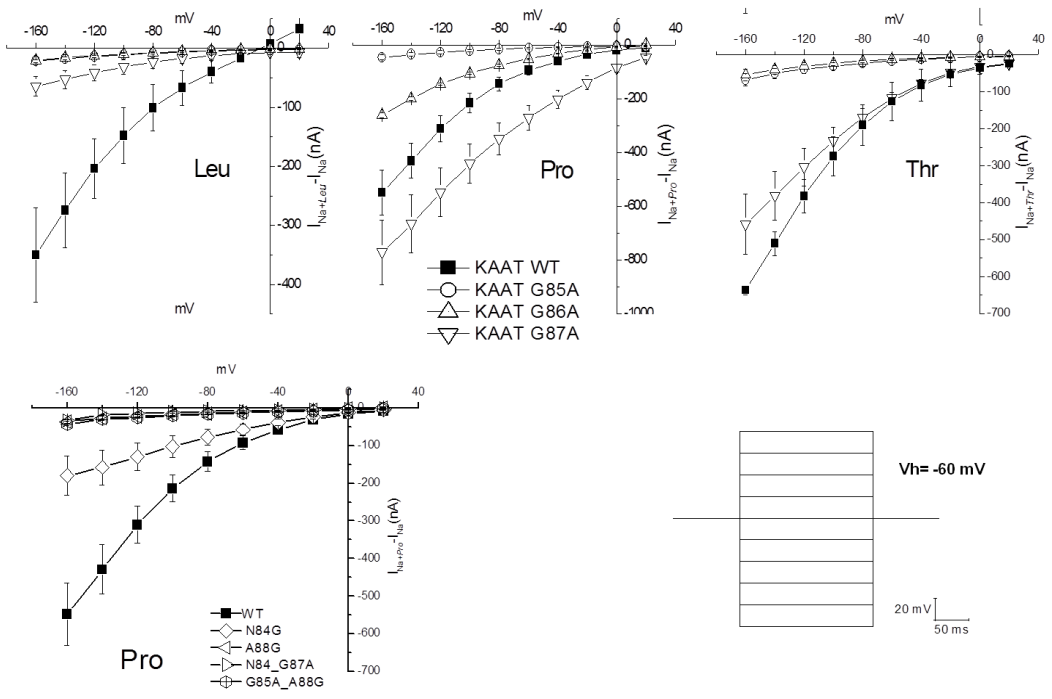

Fig.3.5*: I/V relationships from wt and mutated transporters, in presence of Na^+ and the indicated amino acid. Value are means ± SE from 8 to 10 oocytes in each group. The panel on the right bottom illustrate the pulse protocol applied.*

3.1.3 Estimation of Na^+ apparent affinity

The apparent affinity for Na^+ of the glycine mutants (G85A, G86A; G87A) has even been tested: the transport-associated current elicited by a fixed saturating concentration (3mM) of the substrate threonine was measured in presence of different Na^+ concentrations, from 0.3 to 98 mM. Only the G87A mutant showed a transport activity when the sodium was lower than 1 mM.

The data of the transport current (Fig.3.6), calculated as the difference from the current in the presence and in the absence of amino acid, were normalized to the maximal current in 98mM Na^+, 3mM Thr (Relative inward (-1) current in the graph) and fitted by Logistic equation. The values of the sodium concentrations giving rise to half of the maximal current are indicated in the table inside the Fig 3.5. The Na^+ apparent affinity decreased for the G85A and G86A mutants (K_{50} =64±2.2 and 62±2.8 mM respectively), instead for the G87A mutant this parameter increased (K_{50} =9±1.2 mM), if compared to the wild type (K_{50} = 34±7 mM).

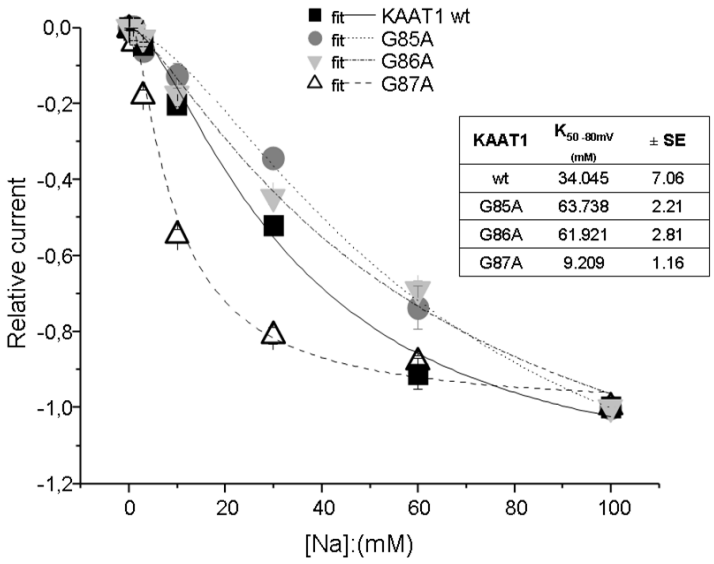

***Fig 3.6**: Apparent affinity for Na^+ in the mutated isoforms: The values of transport current are obtained at -80 mV. In the inset, the table reports the fitting values for the different mutants. The data were from two batches and from 4 to 12 oocytes for each Na^+ concentration.*

The difference in the apparent affinity for Na^+ and the alteration of amino acid uptake and of the transport-associated currents observed in KAAT1 mutants, suggested to investigate if the modification in the glycine triplet could also alterate the interaction with the other KAAT1 driving cations: Li^+ and K^+.

3.1.4 Cation interaction

Although in the presence of Li^+, G87A mutant was able to transport leucine inducing an uptake comparable to that of KAAT1 wt (see Fig. 3.7A), the G86A mutant exhibited a transport activity reduced to 50% of wt while the G85A mutant was inactive.

In order to analyze the transport current in lithium, it has been decided to use the proline as substrate, considering that the leucine elicits a large leak current in the NSS family transporters. In this way it could be showed the transport current as the difference of the current in the presence and in the absence of the substrate. In fact, as reported in (Bossi *et al.*, 2000), the addition of leucine to the Li^+ solution, at negative potential, switches the transporter from the leak mode to the transport mode, blocking the large leak current, so that after the subtraction the resulting transport current shows an "apparent" outward direction. Differently, with the proline, the transport current is larger and the difference gives an inward transport current. The *I/V* relationships (Fig.3.7B) of the transport current here reported in the presence of 100 mM LiCl with 3mM proline confirmed the uptake data obtained in 0.1mM leucine (Fig. 3.6A): G85A was inactive, G86A was similar to the wild type and finally G87A showed a larger current.

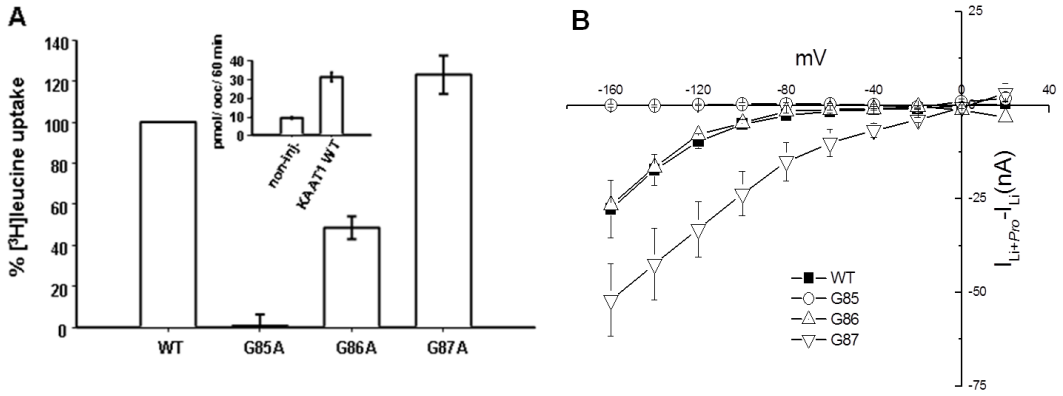

Fig. 3.7*: Amino acid uptake and transport associated currents measured in the presence of a Li+ gradient. A) Data are expressed as percentage of wt and are means ± SE of 30 oocytes from 3 different batches. Inset:0.1 mM leucine uptake measured in KAAT1 wt expressing oocytes or in non injected oocytes as a control. B) Data were obtained by subtracting the traces recorded in the absence from those recorded in the presence of the indicated substrate. Values are means ± SE from 4 to 6 oocytes in each group.*

Analyzing the interaction between the mutants and K^+, it was observed that the G87A mutant showed a transport activity of 150% compared with wt; the G86A mutant activity was reduced to 20% and G85A mutant was inactive (Fig.3.8A).

Data from electrophysiological analysis showed that in the presence of 150 mM KCl, all three mutants exhibit a similar reduced transport current (Fig.3.8B). This apparent discrepancy with the uptake data is due to the transport current estimation that is usually calculated as the difference of the current in the presence from that in the absence of the amino acid. In this case, a larger "leak" or "uncoupled" current compared to wt has been observed in the G87A mutant-expressing oocytes (Fig.3.8). Indeed, in uptake conditions without cell potential control, the high concentration of K^+ generates a depolarization of the membrane voltage until value around 0 mV. It should be noted that under these unfavorable conditions the G87A mutant, which has a lower expression level than wt (Fig.3.1) still exhibits a larger leucine uptake.

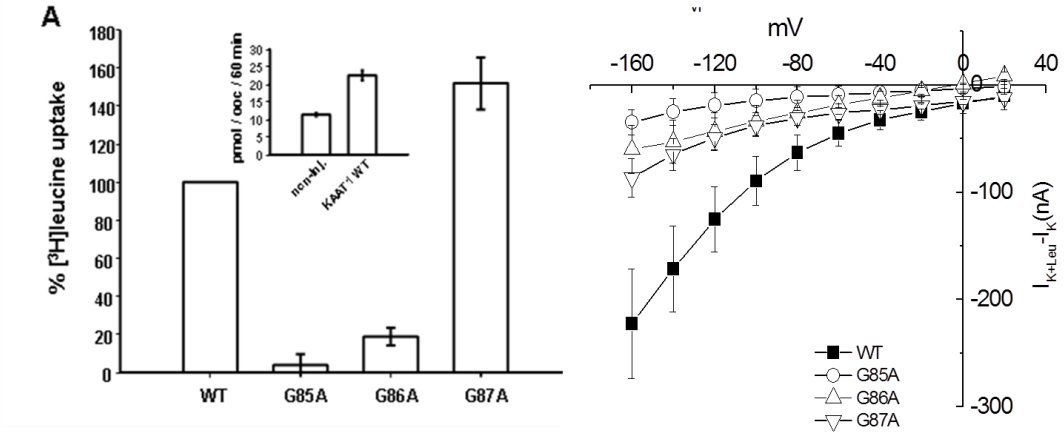

***Fig.3.8**: Amino acid uptake and transport associated currents measured in the presence of high external concentration of K^+. A) Data are expressed as percentage of wt and are means ± SE of 24 oocytes from 3 different batches. Inset: 0.1 mM leucine uptake measured in KAAT1 wt expressing oocytes or in non-injected oocytes as a control in the presence of 150 mM KCl. B) Data were obtained by subtracting the traces recorded in the absence from those recorded in the presence of leucine. Values are means ± SE from 4 to 6 oocytes in each group.*

3.1.5 Leak currents

The determination of the leak currents in KAAT1 and glycine mutants, obtained as the difference between the level in presence of Na^+, Li^+, K^+ (ion solution I-I_{ion}) and the level in TMA^+ solution (Bossi *et al.*, 1999a;Bossi *et al.*, 1999b) led us to two interesting aspects: the leak currents were altered in G85A and G86A mutants, in particular the Li^+ current was close to 0 in the first of them, and reduced in the second. Furthermore, in these two mutants the Na^+ current was lower than in the wt. The G87A had instead the greatest uncoupled currents in all the three tested cations (Fig.3.9).

Non-injected oocytes were tested as controls and, as shown in the figure reported below, no uncoupled current could be detected in solutions containing Na^+ and Li^+, differently from K^+.

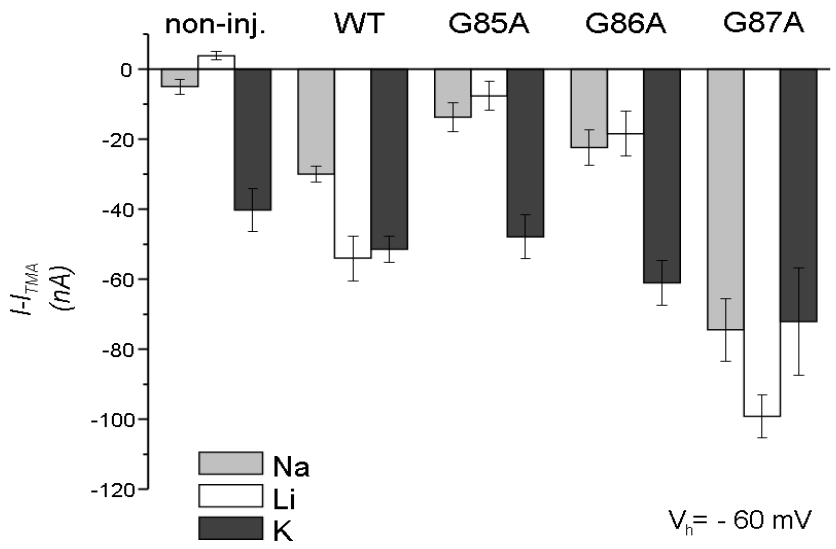

***Fig. 3.9**: Leak currents in KAAT1 and glycine mutants. Oocytes expressing KAAT wt (n=12), glycine mutants (n=14)and non-injected oocyte (n=7). Data represent means ± SE from batches.*

3.2 Temperature effects on the transport activity of ion-coupled cotransporters

Studying the effects of the temperature on the kinetics and amplitude of the transport characteristics represents an useful means to obtain information on the nature of the process, since the temperature coefficient Q_{10} is related to the complexity of the conformational changed involved. It allows to discriminate between the mechanisms generated from diffusional processes (Q_{10} < 1,5) and those involving conformational changes (Q_{10} > 2).

All ion-coupled cotransporters tested so far to analyse the effects of temperature have shown changes in transport activity with Q_{10} values of about 3 or more (Hazama *et al.*, 1997;Binda *et al.*, 2002;Hilgemann & Lu, 1999;Bacconi *et al.*, 2007;Bossi *et al.*, 2012;Broer, 2002).

On the basis of considerations obtained from a recent work in our laboratory, on a mammalian intestinal transporters of oligopeptides PepT1, in which it has been observed

that the apparent substrate affinity was significantly affected by temperature, it has been decided to think of a kinetic interpretation of the substrate affinity in which a greater substrate concentration is required to keep up with the ability of a faster turnover of the transporter.

3.2.1 Apparent affinity changes induced by temperature in KAAT1

The effects of the temperature on substrate affinity have been studied, first, in the amino acid transporter KAAT1 then, in rat neuronal GABA transporter GAT1, originating respectively from two different species, from a poikilotherm inverterbrate the first one, from mammalian animal (homeotherm) the second one.

For KAAT1 experiments, a staircase voltage protocol was used to minimize temperature fluctuations during the recording (Bossi *et al.*, 2012). The protocol was applied from a holding potential (V_h) = -60 mV and the voltage protocol covered in the interval -140 to +20 mV to account for the more negative operating range of this transporter (Bossi *et al.*, 1999b). The staircase consisted of nine 20 mV steps of short duration because the decline of the presteady-state currents is much faster in this transporter. Fig.3.10 illustrates the results of this experiment.

The current traces generated from the same KAAT1-expressing oocytes, in the absence or presence of 1 mM threonine, in response to this protocol at two fixed temperature (20 and 30 °C) are shown in Fig. 3.10A and B; this amino acid used as substrate was been the threonine since it elicits a large transport current in KAAT1 when the driving ion is sodium (Soragna *et al.*, 2004). These currents were strongly accelerated at the highest temperature and, accordingly the transport-associated currents became significantly larger. Dose-response experiments were performed in a series of oocytes at these two temperatures in order to obtain the values of the maximal transport current (I_{max}) and the apparent affinity, in terms of the substrate concentration eliciting the half-maximal current (K_{05}), by fitting the data to the Michaelis-Menten equation:

(eq. 1)

$$I = \frac{I_{max}}{1 + \frac{K_{05}}{[substrate]}}$$

In the Fig. 3.10C and D it is possible to observe the results of this analysis: I_{max} was strongly increased at 30 °C compared to 20 °C, becoming similar to that observed in the oligopeptide transporter PepT1(Bossi *et al.*, 2012); while the Q_{10} values are between 3 and 4.

The effect of temperature on K_{05} is shown in Fig.3.10, panel D: it showed an increase at more positive potentials confirming previous observations (Miszner *et al.*, 2007), concerning the effects of temperature, a significant increase in the value of K_{05} was evident at 30 °C compared to 20 °C.

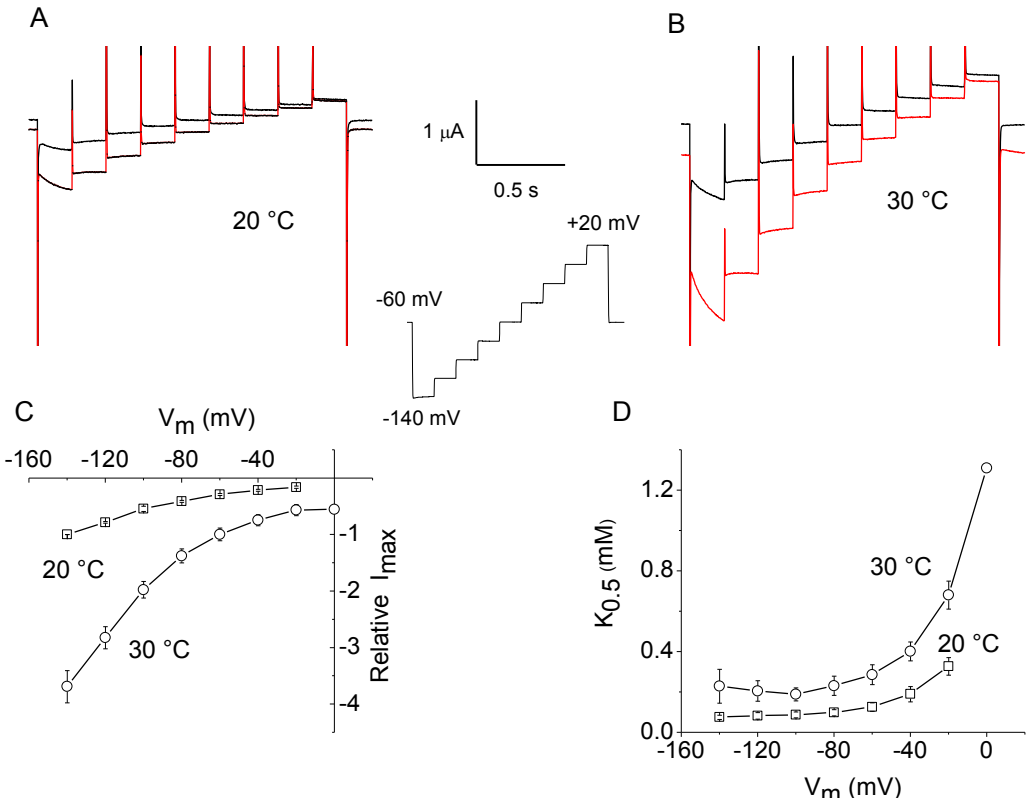

***Fig.3.10**: Temperature effects on the kinetic properties of KAAT1 with threonine as a substrate. Top row: currents in the absence (black) or presence (red) of 1 mM threonine at 20 °C (A) and 30 °C (B) in response to the staircase voltage protocol shown in the inset. The bottom row shows the results of the Michaelis-Menten analysis performed on dose-response curves obtained using the same experimental protocol: voltage dependence of I_{max} (C) and of K_{05} (D) at the indicated temperatures. Data are means ± SE from six oocytes (two batches). The current data were normalized to the value at -120 mV and 20 °C for each oocyte before averaging. Some I_{max} and K_{05} values at the most positive potentials are omitted because their estimate is unreliable. All data at 30 °C (except the K_{05} value at -140 mV) were significantly different ($P < 0.05$) from those at 20 °C (Student's t-test).*

3.2.2 Apparent affinity changes induced by temperature in rGAT1

Previous experiments performed in the insect cotransporter KAAT1, illustrating changing in the apparent substrate affinity related to the increase of the temperature (as observed in PepT1), suggest that this phenomenon might be a common feature, with general relevance on the working mechanism of ion-coupled cotransporters, even belonging to different gene families. To reinforce this notion, the behaviour of another cotransporter belonging to the Na^+/Cl^- family but originating from mammalian (homeotherm) animals, rGAT1, has been tested at the same temperatures in order to compare it with that of the model studied in this thesis.

The same kind of experiment illustrated in Fig.3.10 was repeated on GAT1-expressing oocytes using GABA 300 µM as substrate.

In this case (Fig.3.11), the holding potential was kept at -40 mV and the voltage protocol consisted of five steps, with longer duration compared to those used for KAAT1, because the decline of the presteady-state currents is much slower in this transporter. In fact, it was covered in the range from -120 to +40 mV in 40 mV intervals and the steps were 400 ms in duration to allow the complete decline of the presteady-state currents, particularly at the lowest temperature. The current traces generated from the oocytes in the absence or presence of GABA 300 µM, in response to this protocol at two fixed temperatures (20 and 30 °C) are shown in Fig. 3.11A and B. As expected (Mager *et al.*, 1993;Mager *et al.*, 1996;Forlani *et al.*, 2001), the presteady-state currents visible in the absence of GABA (arrows) were abolished by its addition. Furthermore, as evidenced in KAAT1, even in

rGAT1 the transport associated currents (red colour) were strongly accelerated at the higher temperature and became significantly larger.

Dose-response experiments were obtained in this case as well and the data were analysed with the Michaelis-Menten equation (eq. 1). As illustrated in the Fig. 3.10C and D, raising the temperature from 20 to 30°C produced a considerable increase in $I_{max,}$ which was larger than that observed previously in KAAT1 as well in the oligopeptide transporter PepT1(Bossi *et al.*, 2012).

Indeed, the action of temperature on K_{05} might be seen in the Fig.3.11,panel D: at 20 °C this parameter was voltage-dependent as previously reported (Fesce *et al.*, 2002;Forlani *et al.*, 2001;Mager *et al.*, 1993), and increased at negative potentials, with values between 5 and 20 µM. At 30 °C; in the same oocytes, K_{05} was significantly larger at all potentials, while the voltage-dependence was qualitatively preserved, differently from that exhibited by KAAT1 (Fig.3.10D).

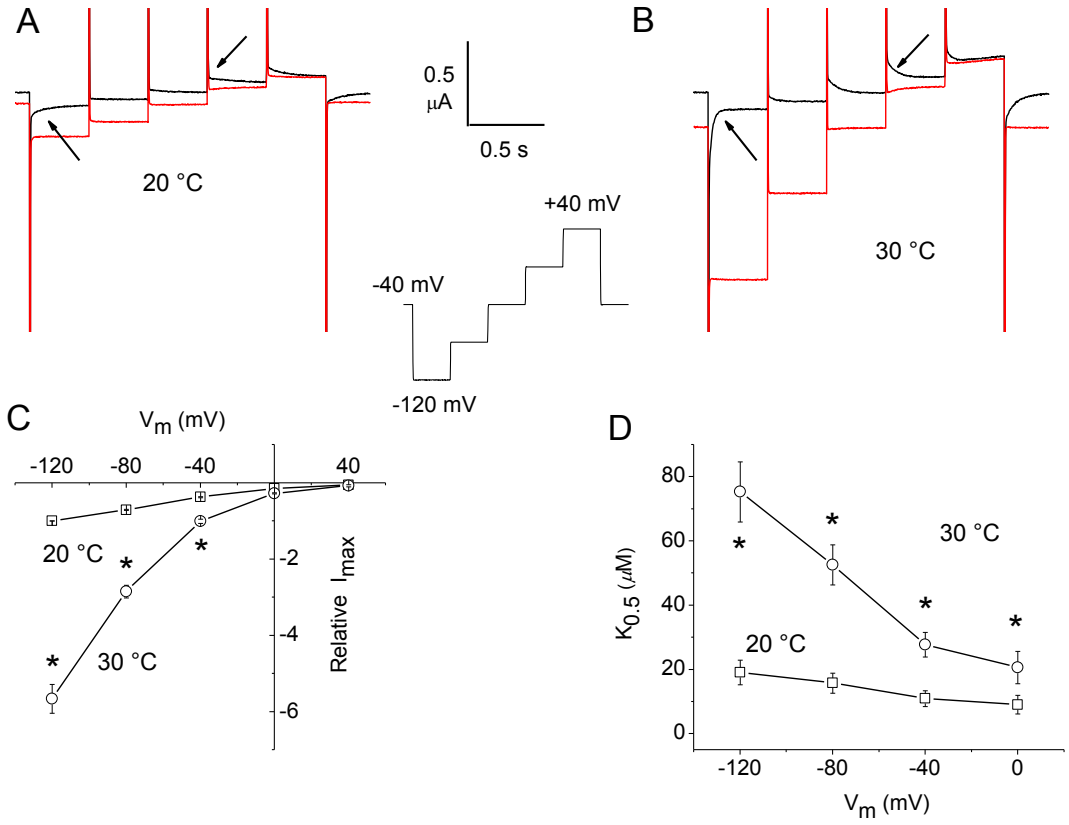

***Fig.3.11**: Temperature effects on the kinetic properties of rRGAT1. Top row: currents in the absence (black) or presence (red) of 300 µM GABA at 20 °C (A) and 30 °C (B), in response to the staircase voltage protocol shown in the inset. The arrows point to the presteady-state currents that disappear in the presence of GABA. The bottom row shows the results of the Michaelis-Menten analysis performed on dose-response curves obtained using the same experimental protocol: voltage dependence of I_{max} (C) and of K_{05} (D) at the indicated temperatures. Data are means ± SE from seven oocytes (three batches). The current data were normalized to the value at -120 mV and 20 °C for each oocyte before averaging. The K_{05} value at +40 mV is omitted because its estimate is unreliable. Data marked with asterisks were significantly different at the two temperatures (Student's t-test, $P < 0.05$).*

3.2.3 Overall efficiency

The increase in I_{max} and the decrease in apparent affinity reported above will be in contrast each other in determining the overall efficiency of the process. This parameter might be estimated, according to enzyme kinetics criteria (Stryer, 1988), as the ratio I_{max}/K_{05}, and it has been plotted in Fig.3.12 (A and B) for the two transporters GAT1 and KAAT1. Our findings demonstrate that in both cases, the transport efficiency increased as the membrane potential was made more negative.

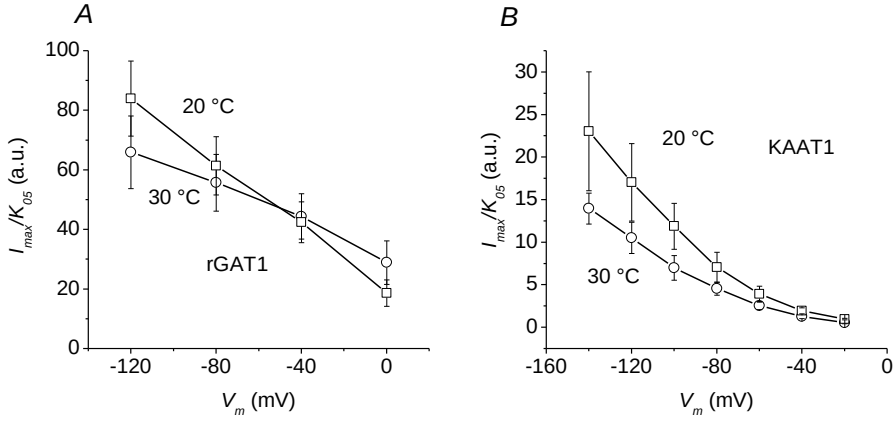

***Fig.3.12**: Temperature dependence of the efficiency of transport. The ratios I_{max}/K_{05} have been calculated from the data in Fig. 3.10C and D for rRGAT1 and from the data in Fig. 3.11C and D for KAAT1. The values are in arbitrary units because of the normalization of the maximal current. Error bars are standard errors of the mean.*

Both transporters did not show any statistically significant difference between 20 and 30°C, especially in the physiological range of membrane potentials, around -70 mV for a neuronal presynaptic membrane, or surrounding glial cells, where rGAT1 is generally located, and at about -200 mV for the luminal side of absorptive intestinal cells, in the case of KAAT1(Dow, J.A.T. & Peacock, J. M.,1989).

Chapter 4

Discussion

4.1 KAAT1: the functional role of the highly conserved glycines triplet

The analysis of the functional characteristics of native and mutated transporters, in general, can give some insight on the molecular mechanisms involved, and in some cases may allow the dissection of different protein functions.

Glycine rotates easily and adds flexibility to the polypeptide chain because of the presence of two hydrogen atoms at the α-carbon. The importance of the flexibility conferred by glycine is proven by the fact that the K^+ channel activation gate involves key identified hinge glycine residues (Chen *et al.*, 2004b), present in the M2 regions of K2P channels; indeed mutations of these glycines in both KCNK0 and in TASK3 (Rudnick & Clark, 1993) led to a reduction in channel open probability.

Furthermore, another evidence about the important role of the studied residues is given by the evidences that glycine-rich elements are described in binding sites of enzymes, such as protein kinases, in which the interaction with variable substrates requires the absence of steric restrictions at the binding site (Bossemeyer, 1994). In 2002, Jiang Y. and co-workers (Jiang *et al.*, 2002) showed that a glycine residue may act as a gating-hinge in potassium channels; other evidences have been presented suggesting that glycine residues engineered into the proton-coupled lactose transporter confer conformational flexibility (Leyland & Dart, 2004).

The high degree of conservation of the glycines residues in NSS transporters suggested a common relevant role in transport function that may be related to conformational flexibility. Data obtained from the analysis of G85, G86 and G87 mutants in KAAT1(Giovanola *et al.*, 2012) support this hypothesis, in fact this sequence is located at the extracellular side of protein, close to one of the residues that participates in the external gate (Arg 30 in LeuT, Arg 76 in KAAT1).

4.1.1 Cell surface expression of glycine mutants

Cell surface expression evaluated by single-oocyte chemiluminescence (SOC) experiments allowed to exclude that the mutations in KAAT1 had caused a defective targeting to the plasma membrane.

The results reported show that although with a variable expression level, glycine-alanine substitutions did not cause an evident alteration of surface localization related to the KAAT1 transporters: the three mutants (N84G, G86A, and A88G) showed an expression comparable to the wild type transporter, while a reduced expression was seen for the three isoforms (G85A, G87A and G85A/A88G). The only exception was represented by the double mutant N84G/G87A, which was undetectable in the oocyte membrane, and obviously did not generate any transport-associated current.

As many intestinal transporters, KAAT1 shows a broad substrate specificity that, in contrast to most mammalian homologues, is influenced by the driving ion (Castagna *et al.*, 1998;Soragna *et al.*, 2004;Miszner *et al.*, 2007). As mentioned in the *Introduction* section, although KAAT1 utilizes K^+ as driver ion for the transport of amino acid, it can also mediate a Na^+ -coupled amino acid transport (and this ion can activate the amino acid transport even at low concentration) and Li^+ (Bossi *et al.*, 1999a;Castagna *et al.*, 1997;Hennigan *et al.*, 1993a).

4.1.2 Analysis of the transport activity of the glycine mutants

A marked reduction of uptake and transport-associated currents has been observed for all the mutants compared with wt, for all tested substrates and in the presence of each of the driver cations of KAAT1. On one hand, it is possible that the low activity of the glycine mutants analysed may reflect their degree of deviation from the native structure.

As demonstrated in Fig.3.2, the only exception was represented by the G87A mutant that although exhibited a 50% reduction of surface expression, showed, in the presence of Na^+, a proline uptake and proline and threonine transport- associated currents similar or even larger than the wt. Furthermore, not only the introduction of alanine increased the ion translocation in the absence of substrate, but this substitution in the presence of proline as substrate, showed also a transporter- dependent uncoupled current (Fig.3.4) (Peres &

Bossi, 2000). This current was observable in presence of both driven and driving substrates and manifested itself as a current in excess to that associated with the stoichiometric charge traslocation (Andrini *et al.*, 2008;Perez-Siles *et al.*, 2011).

In the matter of the behavior of G87A mutant in the presence of Li^+ or K^+, it was ween that it induced a leucine uptake significantly higher than wt protein (Figs.3.7, 3.8).

4.1.3 Leak currents and Cation interaction

Besides the transport-associated current, cotransporters may show one or two types of uncoupled currents (Perez-Siles *et al.*, 2011). The behaviour of these currents was also investigated in the KAAT1 glycine mutants.

It was possible to observe that in all the mutants the leak currents were altered, in particular the Li^+ current was absent in G85A, and reduced in the G86A mutant. The G87A mutant showed instead the greatest current for all the three tested cations (Fig. 3.9). In the presence of K^+, this mutant induced higher amino acid uptake than wt and reduced transport associated currents, revealing a partial uncoupling of amino acid and cation flux. For all the mutants, and in particular for G87A, an altered interaction with cations was therefore observed.

Mutant transport activity was still Na^+ dependent but their apparent affinity for the cation was different from that of the wt: it was reduced for G85A and G86A but increased for G87A (Fig. 3.6). The alteration of the apparent affinity for Na^+ might be explained by changes in the distribution of the inward and outward facing forms of these mutated transporters. These results suggest that TM1, close to the triplet, might play a role in the binding of sodium (Zhou *et al.*, 2004).

4.1.4 Conformational changes: involvement of the Glycine Triplet

The external localization of the glycine stretch, its proximity to the external gate of the transporter, as well as its relevance in KAAT1 interaction with cations (Figs. 3.3; 3.5- 3.9)

suggested that the flexibility conferred by glycines may influence the conformation of the external vestibule of the transporter and alter the ions entrance. This would explain the evolutionary pressure that has determined the degree of conservation of the region.

In a study on four membrane proteins with known tertiary structures the nature and distribution of glycines in transmembrane helices were compared (Cao *et al.*, 1998); helical glycines appear predominantly to play a role as mediators of helix-helix interactions, in particular during conformational changes of membrane-spanning domains. Thus, glycine -100 is potentially involved in a critical TM1-helix interaction needed to take place at some point during translocation (Kristensen *et.al*., 2004).

The analysis of LeuT, in complex with different substrates and inhibitors and computational simulations based on structural data (Yamashita *et al.*, 2005;Singh *et al.*, 2007;Zhao *et al.*, 2011) have highlighted the functional importance of the extracellular vestibule of the transporter, where substrates and inhibitors appear not only to access but also to first interact with the protein.

Site-directed spin labeling and electron paramagnetic resonance have shown that Na^+ favors accessibility to the extracellular vestibule basically through movements of the EL4 and the TM1b segment (Claxton *et al.*, 2010). Na^+ binding increased accessibility at positions in TM1b, TM3 and EL4 that projects into the extracellular vestibule above the S1 site. The glycine triplet flanks the TM1b segment, and may allow its movement.

Taken together, the findings obtained from electrophysiological and uptake studies and those related to the cell surface expression allowed to characterize the roles of the individual determinants or in general of the entire glycine triplet in the transport function of KAAT1.

Interestingly, the data reported in this thesis indicate that Na^+ interacts with KAAT1 at least in two different regions: one located at the glycine loop (direct protection) and the other that should correspond to the internal Na^+ binding sites and that influences the conformation of the glycine loop.

These findings may indicate that the glycine triplet in KAAT1 plays a multifunctional role: Gly 85 and Gly 87 are required for the complete surface expression of the transporter (Fig. 3.2), the entire region is affected by the presence of Na^+ and determines the access of cations to the extracellular vestibule of the transporter (Figs. 3.3; 3.7, 3.8, 3.9). The data presented for the G87A mutant are in agreement with observations made in GAT1

transporter (Zhou & Kanner, 2005), in which the corresponding G80A mutant showed increased apparent affinity for Na^+ and a reduced flexibility that, in the absence of the cation, seemed to conditionally "freeze" the transporter in a state from which it could not further proceed in the transport cycle.

It seems likely that also in other transporter families some of the conserved glycine residues may fulfill a role similar to that of glycine 80 in GAT1, or glycine 87 in KAAT1. However, the role played by the glycine triplet in KAAT1 appears more complex than that observed in GAT1 and SERT (Zhou & Kanner, 2005;Mao *et al.*, 2008) and it might be related to the wider substrate specificity of intestinal amino acid transporters compared with neurotransmitter transporters. Obviously, in order to fully understand and appreciate the biological and pharmacological properties unique to human secondary transporters, the atomic structure of eukaryotic homologues must be obtained.

4.2 Temperature effects on two ion-coupled cotransporters

The possibility of heterologous expression in Xenopus *laevis* oocytes has greatly expanded our knowledge of the properties of several cotransporters. However, in the majority of the cases, the experiments have been performed at room temperature (Forster *et al.*, 2000;Binda *et al.*, 2002;Forster *et al.*, 2006) a situation that, while necessary to keep the amphibian oocytes in optimal condition, is certainly not physiological for the mammalian transporters often used. This limitation prevents a full knowledge of the properties of a mammalian protein under study. Commonly oocytes studies are performed at room temperature (22±2°C), irrespective of the thermoregulation characteristic of the species.

The interest of our experiments to investigate temperature effects on the functioning of two ion-coupled cotransporters originated from different species is two-fold: on one hand to acquire data on the kinetic properties of the system at more physiological temperatures and, on the other, to gain new insights on the molecular processes involved, on the basis of the Q_{10} values.

All ion-coupled cotransporters tested so far to investigate the effects of temperature have shown changes in transport activity with Q_{10} values of about 3 or (Hilgemann & Lu, 1999;Hazama *et al.*, 1997;Beckman & Quick, 2001;Broer, 2002;Binda *et al.*, 2002;Bossi *et*

al., 2012). Just to quickly summarize, Q_{10} values below 1.5 are indicative of diffusional processes, while conformational changes are generally characterised by a stronger temperature dependence and therefore by higher Q_{10} values.

The large effects reported in *Chapter 3* (Section 3.2), imply high activation energies for the rate-limiting step in the process, in the range of several tens of kJ/mole, and confirm therefore that the transport process could involve a relevant conformational change of the protein.

4.2.1 Affinity changes induced by temperature in KAAT1 and rGAT1

For both the cotransporters, the effects of the temperature suggested that the apparent affinity might also be affected.

First, a strong increase in the transmembrane current generated by the presence of the specific substrates, as well a faster decline of the transient currents, was observed at higher temperature (30°C) (Figs.3.10, 3.11, *A* and *B*). As previously reported (Binda *et al.*, 2002), this kind of effect reflects the acceleration in the rate costants of the intramembrane charge movement that underlies these currents. Then, when the maximal transport-associated current (I_{max}) and the apparent substrate affinity (K_{05}) were measured, both transporters showed greater K_{05} values (i.e. a decrease in affinity) at higher temperatures. In particular in KAAT1, a considerable increase in I_{max} was observed (Fig.3.10C); this increase was not as large as in the case of GAT1 (Fig.3.11C), but it was instead similar to that observed previously in the rabbit oligopeptide transporter PepT1(Bossi *et al.*, 2012). Furthermore, in rGAT1, Q_{10} values was higher than those reported before (Binda *et al.*, 2002) however, it might be noted that the previous data were obtained using a fixed GABA concentration and therefore, did not account for changes in apparent affinity.

Concerning the voltage-dependence of K_{05}, it may be noted that this parameter at 20°C (Fig.3.10D) was different from that exhibited by rGAT1 (Fig.3.11D), i.e. it showed an increase at more positive potentials rather than a decrease; in fact this behaviour confirms previous determinations (Miszner *et al.*, 2007) and it is very likely related to the different characteristics of the presteady-state currents in the two transporters (Soragna *et al.*, 2005; Bossi *et al*, 1999) .

These results, confirming the effect already observed in PepT1 (Bossi *et al.*, 2012), suggest that this phenomenon might be a common feature, with general relevance on the working mechanism of ion-coupled cotransporters (Beckman & Quick, 2001), even belonging to different gene families. Furthermore, it should be noted that GAT1, a rat neuronal GABA transporter, belongs to a mammalian (homeotherm) animals, while KAAT1, the neutral amino acid transporter cloned from the gut of the inverterbrate Manduca sexta (Castagna *et al.*, 1998), originates from a poikilotherm animal (Castagna *et al.*, 2009).

As introducted in *Chapter 1*, although clearly not a neurotransmitter transporter, KAAT1 has a significant homology with the mammalian neutral amino acid transporter B^0AT1, another member of the SLC6A family (Boudko *et al.*, 2005;Camargo *et al.*, 2005); in fact, it represents a good model to study the functional mechanisms of transporter belonging to this important family.

The fact that both GAT1, involved in many important physiopathological issues, and KAAT1 (Peres *et al*., 2012) exhibit the same behaviour previously observed in PepT1, confirms similar results reported in an earlier papers on the noradrenaline transporter and on the Drosophila serotonin transporter (Beckman & Quick, 2001). However, it must be also noted that no temperature-induced changes in apparent affinity were observed in the human form of GAT1 (Gonzales *et al.*, 2007).

The observation that the apparent substrate affinity is inversely related to the transport rate suggests a kinetic regulation of this parameter. In addition, the present results indicate that the affinities estimated at room temperature for mammalian cotransporters may not be simply extrapolated to their physiological operating conditions. A possible explanation for this behaviour may be directly found in the transport mechanism which, for the transporters under consideration appears very similar (Fesce *et al.*, 2002;Sala-Rabanal *et al.*, 2006;Renna *et al.*, 2011). In these transporters, the initial steps of the cycle, involving the interaction with the driving ion(s) and the following intramembrane charge movement, precede the binding of the organic substrate. Furthermore, these steps are rate-limiting of the entire transport cycle (Nussberger *et al.*, 1997). Consequently, the lifetime of the conformational state in which substrate binding can occur will be shortened when the turnover rate is increased (e.g. in the present case, by a higher temperature). A shorter life time of this state implies that a higher concentration of substrate will be needed to sustain the high turnover rate, leading therefore to a decreased apparent affinity.

4.2.2 Overall efficiency

The overall efficiency of the co-transporters GAT1 and KAAT1 estimated as the ratio I_{max}/K_{05}, demonstrate that in both cases, increases as the membrane potential is made more negative.

Nevertheless, no statistically significant differences between 20 and 30°C are observed in both transporters, in particular in the physiological range of membrane potentials, around -70 mV for a neuronal presynaptic membrane, or surrounding glial cells, where rGAT1 is generally located, and at about -200 mV for the luminal side of absorptive intestinal cells, in the case of KAAT1 (Dow, J.A.T.& Peacock, J.M, 1989).

However, it must be kept in mind that the lipid membrane composition of the *Xenopus* oocyte is unlikely to be the same of a mammalian or of a *Manduca* sexta cell, and therefore, the present results cannot be directly extrapolated to the respective native conditions in which the transporter physiologically operate. The observations obtained in these studies might lead to the idea that the mammalian transporters, at their physiological body temperature, might be much more efficient in substrate translocation. The overall transport efficiency will obviously depend on the apparent affinity of the transporter for the substrate.

Since the increased I_{max} at higher temperature is counterbalanced by a lower apparent affinity, and the two effects approximately compensate for each other, both in rGAT1 and KAAT1, the efficiency, estimated as the ratio I_{max}/K_{05}, could appears temperature-independent.

In the case of the GABA transporter, the lower apparent affinity at higher temperature is likely to produce consequences on the basal extracellular levels of the neurotransmitter, which are known to be very important in neurological pathophysiology (Richerson & Wu, 2003;Richerson & Wu, 2004).

Chapter 5

Conclusions

The work of my PhD research allowed to identify relevant properties of KAAT1, that in addition to its role in the nutrient transport in the insects, represents a good model for the understanding of the molecular physiology of NSS transporters.

Taken together, the findings obtained from electrophysiological and uptake studies and those related to the cell surface expression allowed to characterize the roles of the individual determinants or in general of the entire glycine triplet in the transport function of KAAT1. The results shown in Fig.3.2 indicate that the behavior of all the glycines mutants tested could fully explain the changes observed in transport activity (Figs.3.3;3.4;3.5). As most intestinal transporters, KAAT1 shows a broad substrate specificity that, in contrast to most mammalian homologues, is influenced by the driving ion (Castagna *et al.*, 1998;Soragna *et al.*, 2004;Miszner *et al.*, 2007); this observation may explain the complex role played by the glycine triplet under study. It allows the initial steps of cation interaction with the transporter; a multifunctional role is also demonstrated by the fact that Gly 85 and Gly 87 are required for the complete surface expression of the transporter (Fig.3.2); moreover, the entire region is affected by the presence of Na^+ and determines the access of cations to the extracellular vestibule of the transporter (Figs.3.3; 3.7; 3.8; 3.9).

Furthermore, the alanine scanning mutagenesis approach supported the hypothesis of a relevant role of the glycine triplet in the transport function, possibly related to conformational flexibility. The importance of the flexibility provided by glycine, an amino acid with no side chain, was proven in the literature (Rudnick & Clark, 1993) as well the high degree of conservation of the triplet among the NSS family members. The external localization of the glycine stretch, its proximity to the external gate of the transporter, as well as its relevance in KAAT1 interaction with cations (Figs. 3.3; 3.5- 3.9) suggested that the flexibility conferred by glycines may influence the conformation of the external vestibule of the transporter (where substrates seem to access and to interact with the protein) and alter the ions entrance. This would explain the evolutionary pressure that has determined the degree of conservation of the region.

The integration of structural and computational analysis of LeuT has originated the conception of two different transport models, one based on a “rocking bundle” of transmembrane helices allowing the alternation of the transporter between an inward facing and an outward facing conformation (Forrest *et al.*, 2008) and the other outlining the

role of an external and an internal gate in controlling the access to the central binding site (Krishnamurthy *et al.*, 2009).

In the first model, TM 1, 2, 6 and 7 form a bundle of four associated helices involved in a rocking movement relative to the other transmembrane domains (scaffold) that allows for conformational transitions; data reported in this thesis indicate that the transport process requires reciprocal movements between TM1 and TM2, that can be allowed by the conserved flexible glycine loop. These observations may be of relevance to other transporter families, many of which contain internal inverted repeats.

In the experiments about the temperature effects it was been possible to acquire a better knowledge of the kinetic properties of the cotransport system at more physiological temperatures. Raising the temperature from 20 (temperature normally used to perform electrophysiological measurement in *X. laevis* oocytes) to 30°C, a strong acceleration of the presteady-state currents as well as a significant increase in the transport-associated currents was produced in both the cotransporters (Figs.3.10 A and B; 3.11 A and B). Changes in transport activity with Q_{10} values bigger than 3 imply high activation energies for the rate-limiting step in the process, in the range of several tens of kiloJoules per mole (kJ/mol) and confirm, therefore, that the transport process must involve a relevant conformational change of the protein.

Moreover, the increase of both I_{max} (stronger in the case of rGAT1) and $K_{0,5}$ (that showed a different voltage-dependence in the two cotransporters under study (Figs.3.10D and 3.11D), confirmed previous observations obtained in the intestinal PepT1 transporter (Bossi *et al.*, 2012), showing an increased transport efficiency at negative potentials. The inverse relationship between the I_{max} and the apparent affinity suggests that the two effects approximately compensate for each other, so that the efficiency, estimated as the ratio $I_{max}/K_{0,5}$, would appear to be temperature-indipendent.

It is possible to conclude that a change in apparent affinity with temperature might be a feature shared by different transporters, even those belonging to diverse gene families.

Finally, the functional and structural similarity of KAAT1 to the mammalian neutral amino acid transporter B^0AT1, member of the SLC6A family, as well to many others members of the same family might allow to utilize this insect cotransporter as a model, in order to promote a better understanding of the functional mechanisms of the Na^+/Cl^--dependent cotransporters implied in neurological pathophysiology.

Bibliography

Abramson, J. & Wright, E. M. (2009). Structure and function of Na(+)-symporters with inverted repeats. *Curr.Opin.Struct.Biol*.

Andrini, O., Ghezzi, C., Murer, H., & Forster, I. C. (2008). The leak mode of type II Na(+)-P(i) cotransporters. *Channels (Austin.)* **2**, 346-357.

Bacconi, A., Ravera, S., Virkki, L. V., Murer, H., & Forster, I. C. (2007). Temperature dependence of steady-state and presteady-state kinetics of a type IIb Na+/P i cotransporter. *J.Membr.Biol.* **215**, 81-92.

Beckman, M. L. & Quick, M. (2001). Substrate and temperature differentiate ion flux from serotonin flux in a serotonin transporter. *Neuropharmacology* **40**, 526-535.

Ben Yona, A. & Kanner, B. I. (2009). Transmembrane domain 8 of the gamma -aminobutyric acid transporter gat-1 lines a cytoplasmic accessibility pathway into its binding pocket. *J.Biol Chem.* **284**, 9727.

Bennett, E. R., Su, H., & Kanner, B. I. (2000). Mutation of arginine 44 of GAT-1, a (Na^+ + Cl^-)-coupled γ-aminobutyric acid transporter from rat brain, impairs net flux but not exchange. *J.Biol.Chem.* **275**, 34106-34113.

Beuming, T., Shi, L., Javitch, J. A., & Weinstein, H. (2006). A comprehensive structure-based alignment of prokaryotic and eukaryotic neurotransmitter/Na+ symporters (NSS) aids in the use of the LeuT structure to probe NSS structure and function. *Mol.Pharmacol.* **70**, 1630-1642.

Binda, F., Bossi, E., Giovannardi, S., Forlani, G., & Peres, A. (2002). Temperature effects on the presteady-state and transport-associated currents of GABA cotransporter rGAT1. *FEBS Letters* **512**, 303-307.

Bismuth, Y., Kavanaugh, M. P., & Kanner, B. I. (1997). Tyrosine 140 of the gamma-aminobutyric acid transporter GAT-1 plays a critical role in neurotransmitter recognition. *J.Biol.Chem.* **272**, 16096-16102.

Bossi, E., Centinaio, E., Castagna, M., Giovannardi, S., Vincenti, S., Sacchi, V. F., & Peres, A. (1999a). Ion binding and permeation through the lepidopteran amino acid transporter KAAT1 expressed in Xenopus oocytes. *J Physiol* **515 (Pt 3)**, 729-742.

Bossi, E., Centinaio, E., Moriondo, A., & Peres, A. (1998). Ca2+-dependence of the depolarization-inducible Na+ current of Xenopus oocytes. *J Cell Physiol* **174**, 154-159.

Bossi, E., Cherubino, F., Margheritis, E., Oyadeyi, A. S., Vollero, A., & Peres, A. (2012). Temperature effects on the kinetic properties of the rabbit intestinal oligopeptide cotransporter PepT1. *Pflugers Arch.* **464**, 183-191.

Bossi, E., Renna, M. D., Sangaletti, R., D'Antoni, F., Cherubino, F., Kottra, G., & Peres, A. (2011). Residues R282 and D341 act as electrostatic gates in the proton-dependent oligopeptide transporter PepT1. *J.Physiol* **589**, 495-510.

Bossi, E., Sacchi, V. F., & Peres, A. (1999b). Ionic selectivity of the coupled and uncoupled currents carried by the amino acid transporter KAAT1. *Pflugers Arch.* **438**, 788-796.

Bossi, E., Vincenti, S., Sacchi, V. F., & Peres, A. (2000). Simultaneous measurements of ionic currents and leucine uptake at the amino acid cotransporter KAAT1 expressed in Xenopus laevis oocytes. *Biochim.Biophys.Acta* **1495**, 34-39.

Bossi, E., Fabbrini, M.S., Ceriotti, A. (2007). Exogenous protein expression in Xenopus Laevis OocyTes. Basic procedure. *In vitro Transcrip. and transl. prot.* 375, 107-131.

Boudko, D. Y. (2012). Molecular basis of essential amino acid transport from studies of insect nutrient amino acid transporters of the SLC6 family (NAT-SLC6). *J.Insect Physiol* **58**, 433-449.

Boudko, D. Y., Kohn, A. B., Meleshkevitch, E. A., Dasher, M. K., Seron, T. J., Stevens, B. R., & Harvey, W. R. (2005). Ancestry and progeny of nutrient amino acid transporters. *Proc.Natl.Acad.Sci.U.S.A* **102**, 1360-1365.

Broer, A., Klingel, K., Kowalczuk, S., Rasko, J. E., Cavanaugh, J., & Broer, S. (2004b). Molecular cloning of mouse amino acid transport system B0, a neutral amino acid transporter related to Hartnup disorder. *J.Biol.Chem.* **279**, 24467-24476.

Broer, A., Klingel, K., Kowalczuk, S., Rasko, J. E., Cavanaugh, J., & Broer, S. (2004a). Molecular cloning of mouse amino acid transport system B0, a neutral amino acid transporter related to Hartnup disorder. *J Biol Chem* **279**, 24467-24476.

Broer, S. (2002). Adaptation of plasma membrane amino acid transport mechanisms to physiological demands. *Pflugers Arch.* **444**, 457-466.

Broer, S. (2006). The SLC6 orphans are forming a family of amino acid transporters. *Neurochem.Int.* **48**, 559-567.

Broer, S. (2008). Amino acid transport across mammalian intestinal and renal epithelia. *Physiol Rev.* **88**, 249-286.

Broer, S. (2009). The role of the neutral amino acid transporter B0AT1 (SLC6A19) in Hartnup disorder and protein nutrition. *IUBMB.Life* **61**, 591-599.

Broer, S. & Gether, U. (2012). The Solute Carrier Family 6. *Br.J.Pharmacol.*

Camargo, S. M., Makrides, V., Virkki, L. V., Forster, I. C., & Verrey, F. (2005). Steady-state kinetic characterization of the mouse B(0)AT1 sodium-dependent neutral amino acid transporter. *Pflugers Arch.* **451**, 338-348.

Cao, Y., Li, M., Mager, S., & Lester, H. A. (1998). Amino acid residues that control pH modulation of transport-associated current in mammalian serotonin transporters. *J.Neurosci.* **18**, 7739-7749.

Caplan, D. A., Subbotina, J. O., & Noskov, S. Y. (2008). Molecular Mechanism of Ion-Ion and Ion-Substrate Coupling in the Na+ -dependent leucine transporter LeuT. *Biophysical Journal* **95**, 4613-4621.

Castagna, M., Bossi, E., & Sacchi, V. F. (2009). Molecular physiology of the insect K-activated amino acid transporter 1 (KAAT1) and cation-anion activated amino acid transporter/channel 1 (CAATCH1) in the light of the structure of the homologous protein LeuT. *Insect Mol.Biol.* **18**, 265-279.

Castagna, M., Shayakul, C., Trotti, D., Sacchi, V. F., Harvey, W. R., & Hediger, M. A. (1997). Molecular characteristics of mammalian and insect amino acid transporters: implications for amino acid homeostasis. [Review] [200 refs]. *Journal of Experimental Biology* **200**, 269-286.

Castagna, M., Shayakul, C., Trotti, D., Sacchi, V. F., Harvey, W. R., & Hediger, M. A. (1998). Cloning and characterization of a potassium-coupled amino acid transporter. *Proceedings of the National Academy of Sciences of the United States of America* **95**, 5395-5400.

Castagna, M., Vincenti, S., Marciani, P., & Sacchi, V. F. (2002). Inhibition of the lepidopteran aminoacid co-transporter KAAT1 by phenylglyoxal: role of arginine 76. *Insect Molecular Biology* **11**, 283-289.

Caterina, M. J., Schumacher, M. A., Tominaga, M., Rosen, T. A., Levine, J. D., & Julius, D. (1997). The capsaicin receptor: a heat-activated ion channel in the pain pathway. *Nature* **389**, 816-824.

Celik, L., Schiott, B., & Tajkhorshid, E. (2008). Substrate binding and formation of an occluded state in the leucine transporter. *Biophysical Journal* **94**, 1600-1612.

Chen, J. G., Sachpatzidis, A., & Rudnick, G. (1997). The third transmembrane domain of the serotonin transporter contains residues associated with substrate and cocaine binding. *Journal of Biological Chemistry* **272**, 28321-28327.

Chen, N. H., Reith, M. E., & Quick, M. W. (2004b). Synaptic uptake and beyond: the sodium- and chloride-dependent neurotransmitter transporter family SLC6. *Pflugers Arch.* **447**, 519-531.

Chen, N. H., Reith, M. E., & Quick, M. W. (2004a). Synaptic uptake and beyond: the sodium- and chloride-dependent neurotransmitter transporter family SLC6. *Pflugers Arch.* **447**, 519-531.

Christensen, H. N. (1990). Role of Amino Acid Transport and Countertransport in nutrition and Metabolism. *Physiol Rev* **70**, 43-77.

Claxton, D. P., Quick, M., Shi, L., de Carvalho, F. D., Weinstein, H., Javitch, J. A., & McHaourab, H. S. (2010). Ion/substrate-dependent conformational dynamics of a bacterial homolog of neurotransmitter:sodium symporters. *Nat.Struct.Mol.Biol.* **17**, 822-829.

Cole, K. S. & Curtis, H. J. (1941). Membrane potential of the squid giant axon during current flow. *J.Gen.Physiol* 24, 551-563.

DeFelice, L. J., Adams, S. V., & Ypey, D. L. (2001). Single file diffusion and neurotransmitter transporter: Hodgkin and Keynes model revisited. *BioSystem* **62**, 57-66.

Dodge, K. & Scott, J. D. (2000). AKAP79 and the evolution of the AKAP model. *FEBS Letters* **476**, 58-61.

Dow, J. A. T. & Peacock, J. M. (1989). Microelectrode evidence for the electrical isolation of goblet cell cavities in *Manduca sexta* middle midgut. *Journal of experimental Biology* **143**, 101-114

Einhauer, A. & Jungbauer, A. (2001). The FLAG peptide, a versatile fusion tag for the purification of recombinant proteins. *J.Biochem.Biophys.Methods* **49**, 455-465

Feldman, D. H., Harvey, W. R., & Stevens, B. R. (2000). A Novel Elecrtogenic AminoAcid Transporter Is Activated by K^+ or Na^+, Is Alkaline pH dependent, and is Cl^--independent. *J Biol Chem* **275**, 24518-24526.

Fesce, R., Giovannardi, S., Binda, F., Bossi, E., & Peres, A. (2002). The relation between charge movement and transport-associated currents in the rat GABA cotransporter rGAT1. *J Physiol* **545**, 739-750.

Forlani, G., Bossi, E., Ghirardelli, R., Giovannardi, S., Binda, F., Bonadiman, L., Ielmini, L., & Peres, A. (2001). Mutation K448E in the external loop 5 of rat GABA transporter rGAT1 induces pH sensitivity and alters substrate interactions. *J Physiol* **536**, 479-494.

Forrest, L. R., Tavoulari, S., Zhang, Y. W., Rudnick, G., & Honig, B. (2007). Identification of a chloride ion binding site in Na+/Cl -dependent transporters. *Proc.Natl.Acad.Sci.U.S.A* **104**, 12761-12766.

Forrest, L. R., Zhang, Y. W., Jacobs, M. T., Gesmonde, J., Xie, L., Honig, B. H., & Rudnick, G. (2008). Mechanism for alternating access in neurotransmitter transporters. *Proc.Natl.Acad.Sci.U.S.A* **105**, 10338-10343.

Forster, I. C., Biber, J., & Murer, H. (2000). Proton-sensitive transitions of renal type II Na(+)-coupled phosphate cotransporter kinetics. *Biophysical Journal* **79**, 215-230.

Forster, I. C., Virkki, L., Bossi, E., Murer, H., & Biber, J. (2006). Electrogenic kinetics of a Mammalian intestinal type IIb na(+)/p (I) cotransporter. *J.Membr.Biol* **212**, 177-190.

Giovanola,M.; D'Antoni,F.; Santacroce,M.; Mari,S.A.; Cherubino,F.; Bossi,E.; Sacchi,V.F.; Castagna,M. (2011) Role of a conserved glycine triplet in the NSS amino acid transporter KAAT1. Biochim.Biophys.Acta **1818,** 1737-1744

Gonzales, A. L., Lee, W., Spencer, S. R., Oropeza, R. A., Chapman, J. V., Ku, J. Y., & Eskandari, S. (2007). Turnover rate of the gamma-aminobutyric acid transporter GAT1. *J.Membr.Biol* **220**, 33-51.

Gouaux, E. & MacKinnon, R. (2005). Principles of selective ion transport in channels and pumps. *Science* **310**, 1461-1465.

Guastella, J., Nelson, N., Nelson, H., Czyzyk, L., Keynan, S., Miedel, M. C., Davidson, N., Lester, H. A., & Kanner, B. I. (1990). Cloning and expression of a rat brain GABA transporter. *Science* **249**, 1303-1306.

Haerteis, S., Krueger, B., Korbmacher, C., & Rauh, R. (2009). The delta-subunit of the epithelial sodium channel (ENaC) enhances channel activity and alters proteolytic ENaC activation. *J.Biol.Chem.* **284**, 29024-29040.

Hazama, A., Loo, D. D., & Wright, E. M. (1997). Presteady-state currents of the rabbit Na+/glucose cotransporter (SGLT1). *J.Membr.Biol.* **155**, 175-186.

Hediger, M. A., Coady, M. J., Ikeda, T. S., & Wright, E. M. (1987). Expression cloning and cDNA sequencing of the Na+/glucose co-transporter. *Nature* 330, 379-381.

Hediger, M. A., Romero, M. F., Peng, J. B., Rolfs, A., Takanaga, H., & Bruford, E. A. (2004). The ABCs of solute carriers: physiological, pathological and therapeutic implications of human membrane transport proteins Introduction. *Pflugers Arch.* **447**, 465-468.

Hennigan, B. B., Wolfersberger, M. G., & Harvey, W. R. (1993a). Neutral amino acid symport in larval Manduca Sexta midgut brush-border membrane vescicles deduced from cation-dependent uptake of leucine, alanine and phenylalanine. *BBA* **1148**, 216-222.

Hennigan, B. B., Wolfersberger, M. G., Parthasarathy, R., & Harvey, W. R. (1993b). Cation-dependent leucine, alanine, and phenylalanine uptake at pH 10 in brush-border membrane vesicles from larval *Manduca sexta* midgut. *Biochim.Biophys.Acta* **1148**, 209-215.

Hilgemann, D. W. & Lu, C. C. (1999). GAT1 (GABA:Na+:Cl-) cotransport function. Database reconstruction with an alternating access model. *J.Gen.Physiol* **114**, 459-475.

HODGKIN, A. L., HUXLEY, A. F., & KATZ, B. (1952). Measurement of current-voltage relations in the membrane of the giant axon of Loligo. *J.Physiol* 116, 424-448.

Hoglund, P. J., Adzic, D., Scicluna, S. J., Lindblom, J., & Fredriksson, R. (2005). The repertoire of solute carriers of family 6: identification of new human and rodent genes. *Biochem.Biophys.Res.Commun.* **336**, 175-189.

Ikeda, T. S., Hwang, E. S., Coady, M. J., Hirayama, B. A., Hediger, M. A., & Wright, E. M. (1989). Characterization of a Na+/glucose cotransporter cloned from rabbit small intestine. *J.Membr.Biol.* 110, 87-95.

Jiang, Y., Lee, A., Chen, J., Cadene, M., Chait, B. T., & MacKinnon, R. (2002). The open pore conformation of potassium channels. *Nature* **417**, 523-526.

Kanai, Y. & Hediger, M. A. (2004). The glutamate/neutral amino acid transporter family SLC1: molecular, physiological and pharmacological aspects. *Pflugers Arch.* **447**, 469-479.

Kanner, B. I. (2003). Transmembrane domain I of the gamma-aminobutyric acid transporter GAT-1 plays a crucial role in the transition between cation leak and transport modes. *J.Biol Chem.* **278**, 3705-3712.

Kanner, B. I. (2006). Structure and Function of Sodium-coupled GABA and Glutamate Transporters. *J.Membr.Biol* **213**, 89-100.

Kanner, B. I., Bendahan, A., Pantanowitz, S., & Su, H. (1994). The number of amino acid residues in hydrophilic loops connecting transmembrane domains of the GABA transporter GAT-1 is critical for its function. *FEBS Letters* **356**, 191-194.

Kanner, B. I. & Zomot, E. (2008). Sodium-coupled neurotransmitter transporters. *Chem.Rev.* **108**, 1654-1668.

Keshet, G. I., Bendahan, A., Su, H., Mager, S., Lester, H. A., & Kanner, B. I. (1995). Glutamate-101 is critical for the function of the sodium and chloride-coupled GABA transporter GAT-1. *FEBS Letters* **371**, 39-42.

Krishnamurthy, H., Piscitelli, C. L., & Gouaux, E. (2009). Unlocking the molecular secrets of sodium-coupled transporters. *Nature* **459**, 347-355.

Kristensen, A. S., Larsen, M. B., Johnsen, L. B., & Wiborg, O. (2004). Mutational scanning of the human serotonin transporter reveals fast translocating serotonin transporter mutants. *Eur.J.Neurosci.* **19**, 1513-1523.

Kristensen, A. S., Andersen, J., Jorgensen, T. N., Sorensen, L., Eriksen, J., Loland, C. J., Stromgaard, K., & Gether, U. (2011). SLC6 neurotransmitter transporters: structure, function, and regulation. *Pharmacol.Rev.* **63**, 585-640.

Lester, H. A., Cao, Y., & Mager, S. (1996). Listening to neurotransmitter transporters. *Neuron* **17**, 807-810.

Leyland, M. L. & Dart, C. (2004). An alternatively spliced isoform of PSD-93/chapsyn 110 binds to the inwardly rectifying potassium channel, Kir2.1. *J.Biol.Chem.* **279**, 43427-43436.

Liu, Z., Stevens, B. R., Feldman, D. H., Hediger, M. A., & Harvey, W. R. (2003). K^+amino acid transporter KAAT1 mutant Y147F has increased transport activity and altered substrate selectivity. *Journal of Experimental Biology* **206**, 245-254.

Loo, D. D., Eskandari, S., Boorer, K. J., Sarkar, H. K., & Wright, E. M. (2000). Role of Cl- in electrogenic Na+-coupled cotransporters GAT1 and SGLT1. *J.Biol.Chem.* **275**, 37414-37422.

Mager, S., Cao, Y., & Lester, H. A. (1998). Measurement of transient currents from neurotransmitter transporters expressed in Xenopus oocytes. *Methods Enzymol.* **296**, 551-566.

Mager, S., Kleinberger-Doron, N., Keshet, G. I., Davidson, N., Kanner, B. I., & Lester, H. A. (1996). Ion binding and permeation at the GABA transporter GAT1. *J.Neurosci.* **16**, 5405-5414.

Mager, S., Naeve, J., Quick, M., Labarca, C., Davidson, N., & Lester, H. A. (1993). Steady states, charge movements, and rates for a cloned GABA transporter expressed in Xenopus oocytes. *Neuron* **10**, 177-188.

Malandro, M. S. & Kilberg, M. S. (1996). Molecular Biology of mammalian amino acid transport. *Annual Review of Biochemistry* **65**, 305-336.

Mao, Y., Mathewson, L., Gesmonde, J., Sato, Y., Holy, M., Sitte, H. H., & Rudnick, G. (2008). Involvement of serotonin transporter extracellular loop 1 in serotonin binding and transport. *Mol.Membr.Biol* **25**, 115-127.

Matskevitch, I., Wagner, C. A., Stegen, C., Broer, S., Noll, B., Risler, T., Kwon, H. M., Handler, J. S., Waldegger, S., Busch, A. E., & Lang, F. (1999). Functional characterization of the Betaine/gamma-aminobutyric acid transporter BGT-1 expressed in xenopus oocytes. *J Biol Chem* **274**, 16709-16716.

McAlear, S. D., Liu, X., Williams, J. B., McNicholas-Bevensee, C. M., & Bevensee, M. O. (2006). Electrogenic Na/HCO3 cotransporter (NBCe1) variants expressed in Xenopus oocytes: functional comparison and roles of the amino and carboxy termini. *J.Gen.Physiol* **127**, 639-658.

Melamed, N. & Kanner, B. I. (2004). Transmembrane domains I and II of the gamma-aminobutyric acid transporter GAT-4 contain molecular determinants of substrate specificity. *Mol.Pharmacol.* **65**, 1452-1461.

Miszner, A., Peres, A., Castagna, M., Bette, S., Cherubino, F., Giovannardi, S., & Bossi, E. (2007). Structural and functional basis of amino acid specificity in the invertebrate cotransporter KAAT1. *J.Physiol* **581**, 899-913.

Montell, C., Birnbaumer, L., & Flockerzi, V. (2002). The TRP channels, a remarkably functional family. *Cell* **108**, 595-598.

Navedo, M. F., Nieves-Cintron, M., Amberg, G. C., Yuan, C., Votaw, V. S., Lederer, W. J., McKnight, G. S., & Santana, L. F. (2008). AKAP150 is required for stuttering persistent Ca2+ sparklets and angiotensin II-induced hypertension. *Circ.Res.* **102**, e1-e11.

Nelson, N. (1998). The family of Na^+/Cl^- neurotransmitter transporters. *Journal of Neurochemistry* **71**, 1785-1803.

Nussberger, S., Steel, A., Trotti, D., Romero, M. F., Boron, W. F., & Hediger, M. A. (1997). Symmetry of H+ binding to the intra- and extracellular side of the H+-coupled oligipeptide cotransporter PepT1. *J.Biol.Chem.* **272**, 7777-7785.

Olivares, L., Aragon, C., Giménez, C., & Zafra, F. (1997). Analysis of the transmembrane topology of the glycine transporter GLYT1. *J.Biol.Chem.* **272**, 1211-1217.

Oliveria, S. F., Dell'Acqua, M. L., & Sather, W. A. (2007). AKAP79/150 anchoring of calcineurin controls neuronal L-type Ca2+ channel activity and nuclear signaling. *Neuron* **55**, 261-275.

Palacin, M., Estevez, R., Bertran, J., & Zorzano, A. (1998). Molecular biology of mammalian plasma membrane amino acid transporters. *Physiol Rev.* **78**, 969-1054.

Parent, L., Supplisson, S., Loo, D. D., & Wright, E. M. (1992). Electrogenic properties of the cloned Na+/glucose cotransporter: II. A transport model under nonrapid equilibrium conditions. *J.Membr.Biol.* **125**, 63-79.

Peres A., Vollero A., Margheritis E., D'Antoni F., Bossi E. (2012). An Inverse Relationship Links Temperature and Substrate Apparent Affinity in the Ion-Coupled Cotransporters rGAT1 and KAAT1. *Int. J. Mol. Sci*. **13**, 15565-15574

Peres, A. & Bossi, E. (2000). Effects of pH on the uncoupled, coupled and pre-steady-state currents at the amino acid transporter KAAT1 expressed in Xenopus oocytes. *J Physiol* **525 Pt 1**, 83-89.

Peres, A., Giovannardi, S., Bossi, E., & Fesce, R. (2004). Electrophysiological insights into the mechanism of ion-coupled cotransporters. *News Physiol Sci* **19**, 80-84.

Perez-Siles, G., Nunez, E., Morreale, A., Jimenez, E., Leo-Macias, A., Pita, G., Cherubino, F., Sangaletti, R., Bossi, E., Ortiz, A. R., Aragon, C., & Lopez-Corcuera, B. (2011). An aspartate residue in the external vestibule of glycine transporter 2 (GLYT2) controls cation access and transport coupling. *Biochem.J.*

Quick, M. & Stevens, B. R. (2001). Amino Acid Transporter CAATCH1 is also an AminoAcid Gated Cation Channel. *J.Bio.Chem.* **276**, 33413-33418.

Rauh, R., Diakov, A., Tzschoppe, A., Korbmacher, J., Azad, A. K., Cuppens, H., Cassiman, J. J., Dotsch, J., Sticht, H., & Korbmacher, C. (2010). A mutation of the epithelial sodium channel associated with atypical cystic fibrosis increases channel open probability and reduces Na+ self inhibition. *J.Physiol* **588**, 1211-1225.

Renna, M. D., Sangaletti, R., Bossi, E., Cherubino, F., Kottra, G., & Peres, A. (2011). Unified modeling of the mammalian and fish proton-dependent oligopeptide transporter PepT1. *Channels (Austin.)* **5**, 89-99.

Richerson, G. B. & Wu, Y. (2003). Dynamic Equilibrium of Neurotransmitter transporter Not just for reuptake anymore. *Journal of Neurophysiology* **90**, 1363-1374.

Richerson, G. B. & Wu, Y. (2004). Role of the GABA transporter in epilepsy. *Adv.Exp.Med.Biol.* **548**, 76-91.

Rudnick, G. & Clark, J. (1993). From synapse to vesicle: the reuptake and storage of biogenic amine neurotransmitters. *Biochim.Biophys.Acta* **1144**, 249-263.

Sacchi, V. F., Castagna, M., Mari, S. A., Perego, C., Bossi, E., & Peres, A. (2003). Glutamate 59 is critical for transport function of the amino acid cotransporter KAAT1. *Am J Physiol Cell Physiol* **285**, C623-C632.

Sala-Rabanal, M., Loo, D. D., Hirayama, B. A., Turk, E., & Wright, E. M. (2006). Molecular interactions between dipeptides, drugs and the human intestinal H+ -oligopeptide cotransporter hPEPT1. *J.Physiol* **574**, 149-166.

Singh, S. K. (2008). LeuT: A prokaryotic stepping stone on the way to a eukaryotic neurotransmitter transporter structure. *Channels (Austin.)* **2**.

Singh, S. K., Yamashita, A., & Gouaux, E. (2007). Antidepressant binding site in a bacterial homologue of neurotransmitter transporters. *Nature* **448**, 952-956.

Soragna, A., Bossi, E., Giovannardi, S., Pisani, R., & Peres, A. (2005). Relations between substrate affinities and charge equilibration rates in the GABA cotransporter rGAT1. *Journal of Physiology* **562**, 333-345.

Soragna, A., Mari, S. A., Pisani, R., Peres, A., Castagna, M., Sacchi, V. F., & Bossi, E. (2004). Structural domains involved in substrate selectivity in two neutral amino acid transporters. *Am J Physiol Cell Physiol* **287**, C754-C761.

Torres, G. E., Carneiro, A., Seamans, K., Fiorentini, C., Sweeney, A., Yao, W. D., & Caron, M. G. (2003). Oligomerization and trafficking of the human dopamine transporter. Mutational analysis identifies critical domains important for the functional expression of the transporter. *J.Biol Chem.* **278**, 2731-2739.

Verrey, F., Ristic, Z., Romeo, E., Ramadan, T., Makrides, V., Dave, M. H., Wagner, C. A., & Camargo, S. M. (2005). Novel renal amino acid transporters. *Annu.Rev.Physiol* **67**, 557-572.

Vincenti, S., Castagna, M., Peres, A., & Sacchi, V. F. (2000). Substrate selectivity and pH dependence of KAAT1 expressed in Xenopus laevis oocytes. *J.Membr.Biol.* **174**, 213-224.

Yamashita, A., Singh, S. K., Kawate, T., Jin, Y., & Gouaux, E. (2005). Crystal structure of a bacterial homologue of Na+/Cl--dependent neurotransmitter transporters. *Nature* **437**, 215-223.

Zerangue, N., Schwappach, B., Jan, Y. N., & Jan, L. Y. (1999). A new ER trafficking signal regulates the subunit stoichiometry of plasma membrane K(ATP) channels. *Neuron* **22**, 537-548.

Zhang, X., Li, L., & McNaughton, P. A. (2008). Proinflammatory mediators modulate the heat-activated ion channel TRPV1 via the scaffolding protein AKAP79/150. *Neuron* **59**, 450-461.

Zhao, Y., Terry, D., Shi, L., Weinstein, H., Blanchard, S. C., & Javitch, J. A. (2010). Single-molecule dynamics of gating in a neurotransmitter transporter homologue. *Nature* **465**, 188-193.

Zhao, Y., Terry, D. S., Shi, L., Quick, M., Weinstein, H., Blanchard, S. C., & Javitch, J. A. (2011). Substrate-modulated gating dynamics in a Na(+)-coupled neurotransmitter transporter homologue. *Nature*.

Zhou, Y., Bennett, E. R., & Kanner, B. I. (2004). The aqueous accessibility in the external half of transmembrane domain I of the GABA transporter GAT-1 Is modulated by its ligands. *J Biol Chem* **279**, 13800-13808.

Zhou, Y. & Kanner, B. I. (2005). Transporter-associated currents in the gamma-aminobutyric acid transporter GAT-1 are conditionally impaired by mutations of a conserved glycine residue. *J.Biol Chem.* **280**, 20316-20324.

Zhou, Z., Zhen, J., Karpowich, N. K., Goetz, R. M., Law, C. J., Reith, M. E., & Wang, D. N. (2007). LeuT-desipramine structure reveals how antidepressants block neurotransmitter reuptake. *Science* **317**, 1390-1393.

Zomot, E., Bendahan, A., Quick, M., Zhao, Y., Javitch, J. A., & Kanner, B. I. (2007). Mechanism of chloride interaction with neurotransmitter:sodium symporters. *Nature* **449**, 726-730.

Zomot, E. & Kanner, B. I. (2003). The interaction of the gamma-aminobutyric acid transporter GAT-1 with the neurotransmitter is selectively impaired by sulfhydryl modification of a conformationally sensitive cysteine residue engineered into extracellular loop IV. *J.Biol Chem.* **278**, 42950-42958.